universität wien

DIPLOMARBEIT

Titel der Diplomarbeit

Histone Modifications and Cellular Plasticity in Vertebrate Limb Regeneration

angestrebter akademischer Grad

Magister der Naturwissenschaften (Mag. rer. nat.)

Verfasser:	Bernhard Geßlbauer
Matrikel-Nummer:	9902668
Studienrichtung (lt. Studienblatt):	Genetik - Mikrobiologie
Betreuer:	Prof. Dr. Franz Wohlrab
Wien, September 2008	

Contents

1. Zusammenfassung

Regeneration von Geweben im Allgemeinen und von Gliedmaßen im Speziellen sind sehr selten unter Vertebraten. Eine Ausnahme bildet der amphibische Schwanzlurch *Notophthalmus viridescens viridescens*, welcher ein aussergewöhnliches regeneratives Potenzial im adulten Stadium besitzt. Nach Amputation einer Gliedmaße, unabhängig von ihrer Lokalisation entlang der proximodistalen Achse, wird das entfernte Gewebe wieder aufgebaut. Dieser Prozess beginnt mit einer lokalen Anhäufung von Mesenchym-ähnlichen Zellen, welche als Blastema bezeichnet werden. Diese Zellen zeigen Stammzellen-ähnliche Eigenschaften und ersetzen das verlorene Gewebe. Das Ziel dieser Arbeit war es den Ursprung dieser blastemalen Zellen zu definieren.
Die meisten Studien über blastemale Vorläufer benutzen Muskelzellen. Diese synzytialen Zellen, vor allem jene nahe der Amputationsstelle, werden mononukleär und beginnen zu proliferieren, ein Ereignis, welches als Dedifferenzierung bezeichnet wird. Bis heute sind die grundlegenden Mechanismen der Dedifferenzierung nicht gänzlich verstanden. In dieser Arbeit untersuchen wir die Beteiligung von Histonmodifizierungen und ihrer katalytischen Enzyme an der Dedifferenzierung.

Histon Methylierungen wurden an früh sich regenerierenden Gliedmaßengeweben untersucht, um Muster zu finden, welche die Dedifferenzierung charakterisieren. Das Hauptaugenmerk lag auf Histon H3 Lysin 9 Methylierung, weil diese Modifikation generell mit inaktiven und daher transkriptionell ruhigem Chromatin einhergeht. Durch Vergleich verschiedener früher Zeitpunkte der Gliedmaßenregeneration wollten wir untersuchen ob signifikante Unterschiede in Bezug auf Demethylierung dieser Markierung entstehen. Unsere Daten geben Hinweis darauf, dass innerhalb der ersten 10 Tage der Gliedmaßenregeneration ein signifikanter Verlust von Histon H3 Lysin 9 Methylierung auftritt.

In einem zweiten Ansatz benutzten wir den Inhibitor Trichostatin A (TSA) um die Beteiligung von Histon-Deacetylasen während der Dedifferenzierung zu untersuchen. In vitro kultivierte Molch und Säugetier Muskelzellen wurden unterschiedlichen Konzentrationen von und Inkubationszeiten mit TSA ausgesetzt. Die Resultate deuten darauf hin, dass TSA eine Veränderung induziert, welche die Muskelzellen zur Fragmentierung anregt. Jedoch waren ihre

Spaltprodukte weder mononucleär noch konnte ein Wiedereintritt in den Zellzyklus beobachtet werden.

2. Abstract

Regeneration of tissues in general and limb regeneration in particular is a very rare event among adult vertebrates. An exception is the amphibian urodele *Notophthalmus viridescens viridescens* who displays a remarkable regenerative potential even as an adult. After amputation of the limb, independent of the location along the posterio-distal axis, the removed tissue is rebuilt. This process is initiated by the local accumulation of mesenychmal like cells, referred to as blastema. These cells exhibit stem cell-like properties and give rise to the lost tissue. The emphasis of this work was to find out the origin of these blastemal cells.

Most studies of blastemal progenitors use muscle cells. These syncytial cells become mononucleated and start to proliferate next to the amputation site, an event termed dedifferentiation. To date, the underlying mechanisms of dedifferentiation are not fully understood. In this work we investigated the involvement of histone modifications and their catalytic enzymes during dedifferentiation.

Histone methylation marks were analysed on early regenerating limb tissues to find patterns that characterise dedifferentiation. We focused on histone H3 lysine 9 methylation because this mark is generally associated with inactive and thus transcriptionally silent chromatin. By comparing different early time-points during limb regeneration we wanted to investigate if significant changes arise in terms of de-methylation. Our data indicate that within the first 10 days of limb regeneration a significant loss of histone H3 lysine 9 methylation occurs.

In a second approach we used the small molecule inhibitor Trichostatin A (TSA) to investigate the involvement of histone deacetylases during dedifferentiation. *In vitro* cultured newt and mammalian myotubes were exposed to various concentrations and incubation times of TSA. Our results indicate that TSA induces an alteration, which forces cultured myotubes to undergo fragmentation. However, their progeny were neither mononucleated nor could cell cycle re-entry be observed.

3. Introduction

3.1 Newts

Newts belong to the family of salamanders although they exhibit several specific characteristics. One difference between newts and the other members of the salamander family is their complex life cycle. The development of newts comprises three distinct stages separated by two complete metamorphoses. To date, three different species of newts are used in experimental biology: The red spotted newt *Notophthalmus viridescens viridescens*, from North America, the Iberian newt, *Pleurodeles waltl* and the Japanese newt, *Cynops pyrroghaster*.

3.1.1 Notophthalmus viridescens viridescens

Notophthalmus viridescens viridescens (*N. v. viridescens*), the red spotted newt, belongs to the species of the eastern newt (*Notophthalmus viridescens*). The generic name *Notophthalmus* originates from the Greek and is composed of *notos*, for back, and *ophatalmos*, for eyes. This refers to the typical eye-like red spots outlined in black on the back of the adults of *N.v. viridescens* the nominate form of the subspecies. *Viridescens* is Latin and points out the greenish body colour of most specimen. Four recognised subspecies exist within the species of *N. viridescens*: *N. v. viridescens* (Red-spotted newt), *N. v. dorsalis* (Broken-striped newt), *N. v. louisianensis* (Central newt) and *N. v. piaropicola* (Peninsula newt).

3.1.2 Habitat

The natural habitat of *N. viridescens* is the east coast of the nearctic region, ranging from Florida to the Canadian Maritime Provinces (Riemland, 2000) (see Fig. 1).

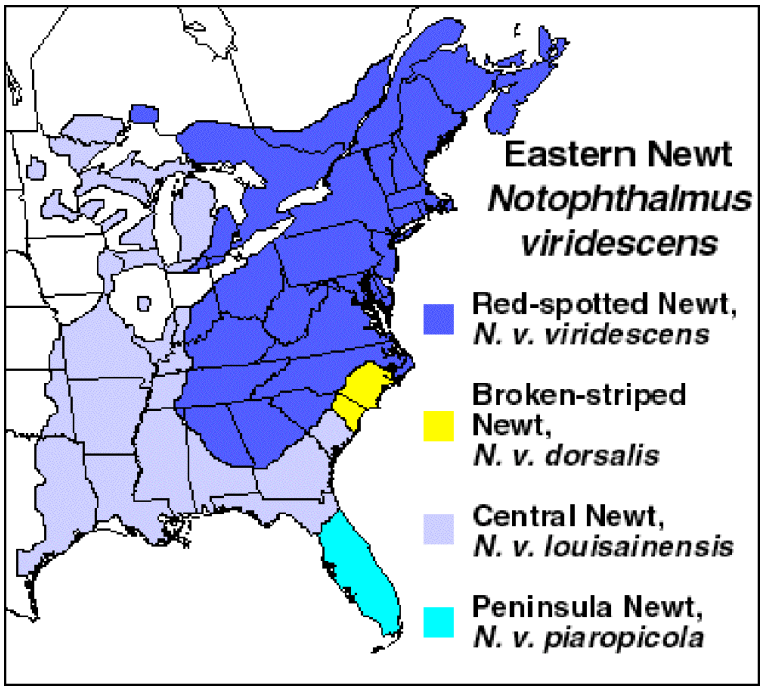

Figure 1. Illustration of the Distribution of the Four Subspecies of *Notophthalmus viridescens*

(Figure taken from http://www.npwrc.usgs.gov; December 5, 2007; 11:41 pm)

3.1.3 Reproduction and life cycle

Notophthalmus viridescens viridescens differ from other salamander in their 3 distinct developmental stages: Aquatic larval, terrestrial juvenile and semi-aquatic adult.

Male newts have 3 behavioral options for inseminating females (Pinou et al., 2000-2002b). The most prominent in nature is an active competition for females as males normally outnumber females at breeding sites. Therefore, females are at first unresponsive to males who begin wooing with nudging the female's cloaca and displaying by twitching and undulating their bodies. After a wooing-ceremony, which can last for several hours, the male newt deposits a spermatophore. After that he leads the female into a position so that her cloaca rests above the spermatophore to collect the sperm cap.

The second insemination strategy is interference. Once the male embraces the female in the so-called amplexus, rival males try to dislodge the male and replace him. Furthermore, competing males can assume the behaviour of breeding females during the spermatophore deposition stage.

Thus, by inserting himself between the courting male and female, the rival manages to deposit his own spermatophore (livingunderworld.org, ; Pinou et al., 2000-2002b).

The third insemination tactic or hula display has mainly been observed in the laboratory. The female is already responsive to the male's initial approach and does not try to evade him. Therefore, he simply performs an undulating dance in front of the stationary female, followed by the deposition of the spermatophore, as soon as the female nudges his cloacal region (livingunderworld.org, ; Pinou et al., 2000-2002b).

Oviposition can take up to several months for a single female newt because they lay up to 400 eggs. Furthermore, the eggs are usually deposited one by one and may be folded into a leaf for protection or are attached to the stems of aquatic plants. The eggs of *N. viridescens* are the smallest among salamanders. An elliptical capsule, consisting of several semipermeable, gelatineous layers, protects the ovum in its centre. Freshly deposited eggs have a diameter of 2.4 to 3.6 mm and quickly swell in water (livingunderworld.org, ; Pinou et al., 2000-2002b).

Larvae hatch about 20-35 days after oviposition. The hatchlings have external gills and short blunt front limbs while the hind legs are absent (Pinou et al., 2000-2002b). Larval newts are aquatic and metamorphosis into terrestrial juveniles occurs after 2-5 months. The size and the timing of metamorphosis into terrestrial juvenile vary between different locations and seem to be influenced by the competition between larvae at high larval density (Hunsinger and Lannoo, 2007).

The sexually immature, terrestrial juvenile stage is also called eft. Efts leave the aquatic environment and migrate into upland forests. They are diurnal and nocturnal (Hunsinger and Lannoo, 2007).
Furthermore, during this terrestrial stage the newts have a brilliant colouring. This coloration is aposematic, meaning that it serves as warning of toxicity for potential enemies (Pinou et al., 2000-2002a). After 2 to 7 years, depending on size and location, efts undergo a less severe metamorphosis into semi-aquatic adults (Hunsinger and Lannoo, 2007; livingunderworld.org).

Sexually mature adults are typically semi-aquatic and prefer slow moving or permanent water bodies. The only remnants of the bright eft coloration are 3-8 orange-red dorsolateral spots outlined in black. Furthermore, skin toxicity is ten times reduced in adult newts. The average life span of adults is 3-8 years (Hunsinger and Lannoo, 2007).

The terrestrial eft stage can also be skipped. Such individuals can go through complete metamorphosis into adults. However, some may develop into neotenes which, in eastern newts, are characterised by the presence of remnants of external gills (Hunsinger and Lannoo, 2007; livingunderworld.org). The neotenous life cycle could be a response to suboptimal terrestrial conditions or ideal aquatic growth conditions such as low larval density, low risk of predation and high abundance of food (Pinou et al., 2000-2002b).

3.1.4 Newts in research

Newts in general, contribute to a wide range of findings in basic research because they offer large cells, nuclei and chromosomes including the particularly interesting lampbrush chromosomes in growing oocytes (Brockes and Kumar, 2005a). For example, the embryonic organiser was discovered in newt embryos by Hans Spemann and Hilde Mangold. The first visualisation of transcription was based on DNA from newt eggs (Miller and Beatty, 1969) and it was demonstrated with DNAse digestion kinetics of newt lampbrush chromosomes that one chromatid consists of a single DNA double helix (Gall, 1963). Furthermore, newts exhibit a remarkable regenerative potential even as adults. They can regenerate their limbs and tails, including spinal cord and sensory ganglia, upper and lower jaws, eye tissue, such as lens and retina, their intestine and small parts of their heart (Brockes and Kumar, 2005a; Brockes and Kumar, 2002). Furthermore, Parish et al. (2007) recently reported that *N. v. viridescens* is also capable of regenerating dopaminergic neurons in a Parkinson-like newt model (Parish et al., 2007). This enormous regenerative potential of newts seems to be unique even among other species capable of regeneration.

These different regeneration-competent organs found in the newt seem to share a common mechanism of plasticity of the differentiated state. Apart from this, there exists no universal

progenitor and different organs use different regenerating mechanisms. For example, the newt heart regenerates by partial reversal of differentiated cardiomyocytes into the dedifferentiated state. Newt cardiomyocytes in the vicinity of a removed apical region of the ventricle proliferate and restore the lesion. Experiments performed in vitro revealed the reactivated cardiomyocytes retain their morphological characteristics despite cell cycle re-entry and cytokinesis (Bettencourt-Dias et al., 2003) . On the other hand, lens regeneration is accomplished from cells of the dorsal pigmented epithelium of the iris. Following lentectomy, cells at that location lose their pigmentation, proliferate and transdifferentiate into lens cells, which in turn build up the new lens. This property is exclusive the dorsal region of the iris. Ventral pigmented epithelial cells fail to restore the lens (Grogg et al., 2005). Limb regeneration in turn, proceeds through an initial step. A mesenchymal mass of cells at the distal portion of the remaining limb stump tissue, also referred to as blastema, originates from several differentiated progenitors. These blastemal cells give rise to all the lost structures and reconstitute the limb. To date, the origin of these blastemal cells is rather unclear (Brockes, 1997; Ferretti and Brockes, 1991; Tanaka, 2003).

Although some other salamander species, such as the axolotl, also possess excellent regenerating skills, they cannot, for example, regenerate their lens (Brockes and Kumar, 2005a).

Even though newts possess unique biological properties and their contributions to our understanding in molecular biology is immense, they play a subordinate role in routine laboratory work. This is due to the fact that they display a complex and long life cycle. Genetic manipulations would last too long to get an investigatable phenotype.
Furthermore, newts have a huge genome size (Straus, 1971)where repetitive sequences seem to occupy most of the genome. Genome sequencing has therefore not been carried out so far, which is a major disadvantage.

3.2 Limb regeneration

In general, regeneration can be classified as either epimorphosis or morphallaxis. The latter one is characterised by a drastic remodelling of the remaining tissue to regenerate the lost body part.

This kind of regenerative mode it widely spread throughout the metazoan phylum e.g. in the hydra and the planarian worm.
In contrast to this, epimorphic regeneration proceeds without remodelling of the remaining tissue, at least it is restricted to the tissue next to the amputation plane. Establishment of the lost body part occurs like an "add-on" process through local formation of a growth zone or blastema at the site of amputation. Limb regeneration resembles epimorphic regeneration.

3.2.1 Stages of fore limb regeneration

The process of limb regeneration can be divided into 3 major phases. Each phase is characterized by specific stages. A total of 11 stages can be distinguished by morphological and histological aspects. The following outline of the stages of fore limb regeneration was obtained from Iten and Bryant (1973):

Wound healing is the first stage of the regeneration process (0-5 days after amputation) (Iten and Bryant, 1973). Instantly after tissue removal the wound surface is closed by a fibrin clot. After 24 hours the distal portion of the stump becomes swollen and the wound surface is already covered with a thin transparent wound epidermis (Iten and Bryant, 1973). Around 3 days after amputation, the wound epidermis is twice as thick (5-7 cells) as the stump epidermis in histological sections. Furthermore, the nerves seem to degenerate at their distal ends (Iten and Bryant, 1973).

The period of 6-8 days after amputation is an "early dedifferentiation stage" (Iten and Bryant, 1973). It is characterised by a kind of swollen and translucent wound surface, which appears to be blister-like (Iten and Bryant, 1973). Histological alterations involve a further increase in thickness of the basement membrane-free apical wound epidermis to 6-11 cells in contrast to 3-4 cells of the stump epidermis (Iten and Bryant, 1973). First signs of dedifferentiation are visible. This is evident through short segments of myotubes containing single nuclei in the vicinity of the wound. Additionally, the first blastemal cells can be detected beneath the apical epidermis (Iten and Bryant, 1973).

The third stage lasts until 11 days after amputation and represents a “late dedifferentiation stage” (Iten and Bryant, 1973). Because of a small blister-like swelling, the distal outline of the stump is roundish (Iten and Bryant, 1973). In histological sections, dedifferentiation of muscle, bone, and degenerating nerves can be observed. The space beneath the apical epidermis is entirely filled with loosely arranged blastemal cells (Iten and Bryant, 1973).

Phase I in the forelimb regeneration process comprises these first three stages. This phase takes a central role in basic research. In summary, differentiated specialised precursor cells form mesenchymal-like cells displaying stem cell properties in a process termed dedifferentiation. These cells, referred to as blastemal cells, cumulate beneath the wounded epidermis and are the basis for the reconstitution of the lost limb part. They will redifferentiate into muscle, cartilage, bone and connective tissue.
Therefore, the underlying mechanisms are of great interest for regenerative medicine. Identifying the underlying genes/factors, their activation and how they control the establishment of the “stem cell” population may render embryonic stem cells dispensable for cells therapy.

The events to follow seem to recapitulate the embryonic development of a limb (Simon and Tabin, 1993). Phase II includes blastema accumulation and blastema growth whereas phase III comprises differentiation and morphogenesis.

During the “moderate early bud stage” (10-14 days after amputation) the localised swelling disappears (Iten and Bryant, 1973). The blastema increases in size and already becomes vascularised. Dedifferentiation within the stump tissues is still proceeding (Iten and Bryant, 1973).

The next stage in limb regeneration is the “early bud stage” (12-17 days after amputation) (Iten and Bryant, 1973). The regenerate is still colourless and the limb stump is dome-shaped (Iten and Bryant, 1973). Dedifferentiation still continues and expands to more proximal stump tissue (Iten and Bryant, 1973).

The sixth stage is called “medium bud stage” (14-20 days after amputation) (Iten and Bryant, 1973). The regenerate appears now cone-shaped and the apex can be either rounded or pointed. For the first time, blood flow can be seen within the blastema from without (Iten and Bryant, 1973).
The blastema appears as a dense aggregation of cells and dedifferentiation is still in progress (Iten and Bryant, 1973).

The “late bud stage” (18-24 days after amputation) (Iten and Bryant, 1973) follows, during which the distal portion of the cone apex flattens dorso-ventrally. Afterwards, a bend develops at the stump-regenerate-border causing the regenerate to point anteriorly (Iten and Bryant, 1973). Histological sections reveal the presence of melanophores within the blastema. For the first time chondrogenesis is visible in the proximal part of the regenerate around the distal part of the bone. Dedifferentiation is no longer detectable (Iten and Bryant, 1973).

A flattened and paddle-like appearance of the distal tip of the regenerate is the morphological characteristics of the “palette stage” (22-28 days after amputation) (Iten and Bryant, 1973). The border of the amputation plane is no longer noticeable after the pigmentation of the regenerate epidermis has reached a certain level (Iten and Bryant, 1973). Chondrogenesis proceeds to radius and ulna, and myogenesis occurs in the proximal part of the regenerate. Blastemal cells are still surrounding the newly formed structures resulting from chondrogenesis and myogenesis (Iten and Bryant, 1973).

Digit formation occurs during the “early digits stage” (24-33 days after amputation) (Iten and Bryant, 1973). The stump is no longer swollen (Iten and Bryant, 1973). The regenerate epidermis is reduced in thickness to 4-6 cell layers. However, the distal epidermis is an exception, as it appears to project deeply into the interdigital tissue. At this stage, skin glands start to develop in the proximal regenerate. By the time of emergence of the first 3 digits, the zeugopodium (radius and ulna) is still connected with the autopodium (Iten and Bryant, 1973).

At the “medium digits stage” (30-40 days after amputation) all four digits are present and begin to separate from each other (Iten and Bryant, 1973). Cartilage, muscle, and connective tissue

dominate within the regenerate. The few residual blastemal cells are mainly in the distal regions of the autopodium (Iten and Bryant, 1973).

Limb regeneration is concluded with the “late digits stage” (34 days after amputation) (Iten and Bryant, 1973). All digits are separated, elongated, and pointed (Iten and Bryant, 1973). The epidermis of the regenerate has the same amount of layers as the stump epidermis (Iten and Bryant, 1973). Differentiation is completed and ossification takes place in peripheral regions (Iten and Bryant, 1973).

Different levels of amputation, through stylopodium or zygopodium, do not affect the overall process of regeneration. From each level of amputation all phases of regeneration are passed at approximately the same time. A difference arises only by the onset of the third phase. Regenerates from a more proximal level along the proximo-distal axis will increase the rate of growth and length compared to regenerates at a more distal level of amputation. Thus, the total length of the regenerate is usually reached at approximately the same time independent of the level of amputation (Iten and Bryant, 1973).

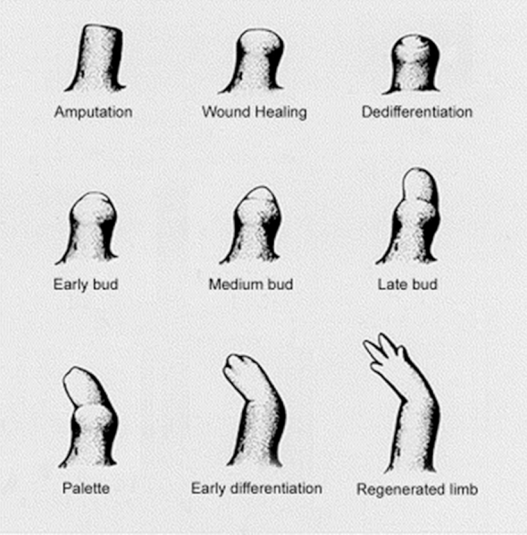

Figure 2. Levels of Fore Limb Regeneration of *Notophthalmus Viridescens Viridescens*
Each stage is characterised by specific morphological and histological alterations (see Section 3.2.1).

(Picture from (Kumar et al., 2007a))

3.3 Blastema

Already 3 days after amputation of the limb, mesenchymal cells start to accumulate beneath the wound epidermis. These mesenchymal cells, also referred to as blastema, give rise to the lost tissue and rebuild the limb. Blastemal cells only reconstitute the lost part of the limb, depending on the actual site/location of amputation. This fact presupposes that blastemal cells inherit positional information concerning the proximodistal axis from their ancestors/precursors. Blastema graft studies verified this hypothesis. Transplantation of a particular blastema from a specific level along the proximodistal axis to the dorsal fin or anterior chamber of the eye resulted in corresponding to limb structures at the site of implantation. This feature of the blastema is called positional memory and points out its self-organizing properties, which means that blastemal cells are independent of any templating or inductive activities of the limb stump (Brockes, 1997; Brockes and Kumar, 2005b).

The positional identity of blastemal cells is mediated among other molecules by Prod 1. Prod 1 is a small protein anchored at the cell surface establishing a gradient along the proximodistal axis. It was identified after studies had revealed that retinoic acid could re-specify distal blastemal cells to a more proximal identity (da Silva et al., 2002).
Investigations to characterise a binding partner of Prod 1 yielded nAG (newt anterior gradient) protein as a secreted ligand for Prod 1. Expression of nAG in the regenerating nerve sheath (built up by Schwann cells) and wound epidermis depends on an intact nerve in the limb stump. If the brachial nerve is cut before amputation, nAG is not expressed anymore and limb regeneration arrests in an early step. Ectopic expression of nAG in the distal stump tissue starting 5 days post amputation circumvents the presence of an active nerve. Furthermore, nAG enhances proliferation of cultured newt blastemal cells when added to the culture medium containing 1% serum. Therefore, Kumar et al., (2007b) concluded that nerve dependent expression of nAG functions to stimulate proliferation of blastemal cells rather than to have direct effects on their positional specification (Kumar et al., 2007b).

The characterisation of nAG was a first explanation why the early steps of regeneration, particularly from late phase I to the early stages of phase II, are dependent on nerve supply. More

precisely, not the emergence of blastemal cells but their proliferation is directly linked to an intact nerve. The outgrowth of the developing limb bud, on the contrary, proceeds in the absence of axons. However, when the migration of brachial axons into the embryonic limb bud is prevented, regeneration in adult newts is no longer nerve-dependent. Accordingly, innervation of the embryonic limb bud appears to establish nerve dependence in adult limb regeneration. However, the molecular mechanisms underlying this latter phenomenon are not understood today (Ferretti and Brockes, 1991).

3.3.1 Progenitors of the blastemal cells

A central question of epimorphic limb regeneration is the origin of the blastemal cells. Histological analysis of early regenerative tissue gave first hints that muscle cells next to the amputation plane contribute to the mesenychmal cells that build up the blastema. Syncytial muscle cells appeared to have constrictions around their nuclei which would bud off and migrate distally to contribute to the mass of progenitor cells which build up the regenerate (Thornton, 1938).

The usage of monoclonal antibodies (mab) against regeneration- and tissue specific antigens, brought new insights concerning the precursors of blastemal cells. The mab 22/18 specifically recognizes a regeneration specific intermediate filament (Kintner and Brockes, 1984). However, the intermediate filament is not an exclusive structure in blastemal cells, but rather a conformational change in emerging blastemal cells (Ferretti and Brockes, 1990). Next to 22/18, Keratin 8 and Keratin 18 mark blastemal cells, although they are also expressed in glands, blood vessels and perinerium (perichondrium) in normal limb tissue. Another difference between them is that the antigen of mab 22/18 already appears 36-48 hours after amputation whereas the expression of Keratin 8 and Keratin 18 only starts 3 days after amputation (Ferretti and Brockes, 1991).

The combination of 22/18 with different tissue specific markers brought up a number of potential sources of progenitors. Markers of Schwann cells were coexpressed with antigen 22/18 in the most proximal blastema cells. A component of the sarcoplasmic reticulum could be detected in a few 22/18 positive cells and markers of fibroblasts were co-expressed in the majority of

blastemal cells. In contrast, neither epidermal nor wound epidermis-specific markers were co-expressed in 22/18 positive cells (Ferretti and Brockes, 1991).

The origin of blastemal cells could be connected with dedifferentiation. This theory implies that mature, differentiated tissues undergo a transition to an earlier developmental stage. Syncytial muscle gives rise to mononucleated cells while chondrocytes leave the cartilage matrix and Schwann cells exit the myelin sheath to build up the blastemal stem cell mass.

Another origin of blastemal cells could be tissue specific stem cells. Such tissue restricted stem cells have to go through a dedifferentiation process as well, to be able to give rise to cells of different lineages.

Recently, Morrison et al. (2006) could isolate a Pax7 positive cell fraction from in vitro cultured newt single myofibers. Myofibers injected with tracing dye yielded proliferating offspring without the injected label. This observation led to the discovery of newt satellite cells inside the basement membrane of muscle cells. Furthermore, intramuscular injection of BrdU-labeled newt satellite cells prior to amputation verified that these cells contribute to the blastema. Subsequently, the labeled cells differentiated into cartilage and were also detected in the wound epidermis. Differentiation studies in vitro showed the potential of this cell type to differentiate into cartilage, adipocytes and muscle (Morrison et al., 2006).

Furthermore, it is important to consider the quantity of cells contributed to the blastema by the different tissues. Echeverri at al. (2001) found out that a 4 day old axolotl tail blastema consists of 907 blastemal cells. 43% of those are derived from the dermis and 16.5% arise from dedifferentiation of muscle next to the amputation site. The remaining 40.5% are derived from other sources within the stump tissue (Echeverri et al., 2001).

3.4 Dedifferentiation of muscle cells

3.4.1 Dedifferentiation

The transition of the multinucleated muscle cell to mononucleated cell progeny requires changes on the molecular as well as the cellular level (see Fig. 3) (Duckmanton et al., 2005). Dedifferentiation involves transcriptional repressors of genes, which constitute the differentiated state. At the same time other genes are activated that establish the new properties of blastemal cells.

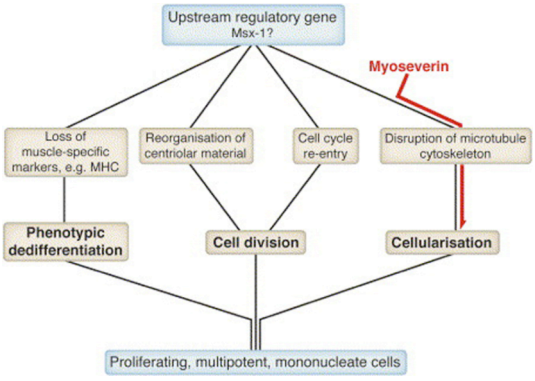

Figure 3. Different Aspects of Muscle Dedifferentiation

This diagram lists steps, which have to be fulfilled to yield mononucleated progeny form syncytial muscle cells.

(Figure from Duckmanton et al., 2005)

Msx-1, a homeobox protein, is suggested to play a central role in the initiation of the dedifferentiation process. Explant cultures of single viable axolotl myofibers displayed a diverse behaviour. Myofibers responding to dissociation were characterised by migration of nuclei within the syncytium and formation of lobulated structures in the middle or at the end of the cell. 10% of the total population of myofibers formed these lobules, containing a single nucleus, which budded off and gave rise to mononucleated cells. Besides these mononucleated cells which could be labeled with tritiated thymidine (a marker for DNA synthesis), 40%-70% of the total population of myofibers gave rise to progeny containing 2 to 3 nuclei. These multinucleated fragments could not be labelled with tritiated thymidine (Kumar et al., 2004).

Fragmenting myofibers responding to dissociation were termed “activated”. Activation was associated with Msx-1 expression whereas non-responding, inactive myofibers did not express Msx-1 (Kumar et al., 2004).

At this point, a brief overview of cellularisation/fragmentation of muscle cells is given to illustrate the possibilities of the origin of mononucleated progeny (see Fig. 4). 4 different possible strategies are known, either comprising an active cell cycle progression or quiescent nuclei (Velloso et al., 2000). Concerning the strategies involving an active cell cycle there are two possibilities.

First, budding could be an effect of mitosis and subsequent cytokinesis.

Second, entry into G1 phase or S-phase could be the inducer to force these "active" nuclei to exit the differentiated environment.

On the other hand, budding has not to be obligatorily linked to active nuclei. It is also possible that under the influence of a certain environment, after tissue injury or in a blastema, nuclei are initially forced to form mononucleated progeny. Afterwards, the derived progeny start to proliferate.

The fourth exit strategy, a variant of the latter one, is the escape of nuclei from a cluster of myotube nuclei. This hypothesis corresponds with observations of osteoclast-like multinucleated giant cells (Velloso et al., 2000).

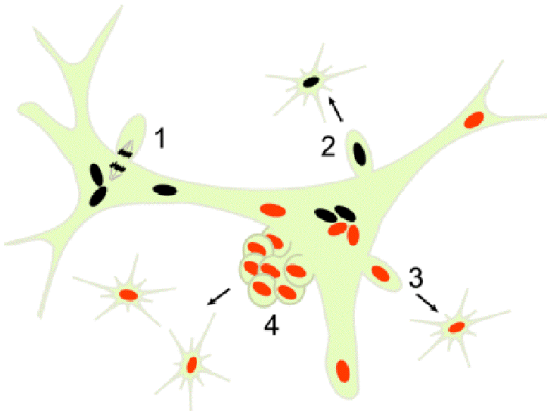

Figure 4. Different Possibilities How Mononucleated Progeny could Originate from Myotubes

Black nuclei re-entered the cell cycle whereas red nuclei are quiescent.

(Figure from (Velloso et al., 2000))

How cell cycle re-entry and cellularisation/fragmentation are connected to each other is not well understood. As described later, cell cycle re-entry occurs without cellularisaton/fragmentation (Tanaka et al., 1997). On the other hand, cultured A1 (a newt myogenic cell line) myotubes, which were blocked for cell cycle re-entry, produce mononucleated offspring when injected into the blastema (Velloso et al., 2000).

Previous studies on mammalian myotubes revealed that terminal differentiation could be overcome by genetic manipulations. Mouse myotubes lacking both copies of the retinoblastoma gene responded to growth factors in the medium by entering the cell cycle (Schneider et al., 1994) .

Viral oncogenes can cause cell cycle re-entry as well. Ectopic expression of SV-40 large T antigen or adenovirus E1A protein induced the nuclei of mammalian myotubes to re-enter the cell cycle. Adenovirus E1A protein expression reduced the levels of muscle-specific proteins, as well, whereas SV-40 large T antigen transfection yielded smaller myotubes or non-proliferating mononucleated cells (Endo and Nadal-Ginard, 1998; Iujvidin et al., 1990).

3.4.2 Cell cycle re-entry by serum stimulation

Cultured A1 newt myotubes are able to re-enter the cell cycle. This feature depends on the phosphorylation of the retinoblastoma (Rb) protein. The Rb protein is a regulator of the G_1/ S restriction point of the cell cycle. It functions as an upstream regulator of E2F transcription factors, which are required to enter S-phase. Phosphorylated Rb protein has a reduced affinity to E2F, so that free E2F is able to initiate S-phase. In mammalian cells, this pathway seems to be exclusive for proliferation sensitive and thus undifferentiated cells. However, newt myotubes retain the ability to respond to elevated levels of serum (from various mammalian sources) by phosphorylation of the Rb protein and thus entering the S-phase. However, cell cycle re-entry was inhibited, if the myotubes were in contact with surrounding mononucleated cells (contact inhibition). The overexpression of a mutant Rb protein lacking the phosphorylation sites prevented newt myotubes to re-enter S-phase. Furthermore, if myotubes were responding to elevated levels of serum in the medium, all their nuclei incorporated BrdU. Thus, cell cycle progression occurs but arrests in G_2 (Tanaka et al., 1997).

Cell cycle re-entry depends on activation of a serum component by thrombin or plasmin. After the addition of thrombin/plasmin (thrombin is more potent than plasmin) to sub-threshold amount of serum-containing medium, S-phase re-entry could be observed. Sub-threshold amount of serum corresponds to 1.5% serum (Tanaka et al., 1999).

This property is not exclusive for newt myotubes. In newt/mouse hybrid cells, mouse nuclei are responsive to serum as well. In this situation the postmitotic arrest of the murine nuclei is overcome by the same pathway that is activated in the newt cytoplasm after serum stimulation (Velloso et al., 2001).

3.4.3 Newt regeneration extract causes dedifferentiation of cultured myotubes

Protein extracts from early blastemal tissue, including blastemal cells and wound epidermis cells, were used to assay their effect on cultured newt and murine myotubes. Purified myotubes from both species cultured in low serum medium were exposed to the protein extract and responded in a comparable fashion (McGann et al., 2001).
25% of newt myotubes re-entered the cell cycle after incubation in regeneration extract and all of the nuclei incorporated BrdU. Cellular cleavage of newt myotubes became apparent between 3-5 days after exposure to the extract. 16% of the cells cleaved to form smaller myotubes or even mononucleated cells (McGann et al., 2001).
64% of responding mouse myotubes re-entered the cell cycle of which only 19% exhibited DNA-synthesis. Cleavage of the cells was observed as well although at the lower level of 11%. Approximately half of the cells resulting from cleavage also started proliferating. Furthermore, the levels of MyoD and myogenin were reduced in the nucleus while the level of troponin T was decreased in the cytoplasm of treated mouse myotubes. MyoD, myogenin and troponin T are markers for terminally differentiated muscle (McGann et al., 2001).

3.4.4 Ectopic expression of msx-1 induces dedifferentiation in murine muscle cells

As described in Section 3.4.1, Msx-1 seems to be a marker of dedifferentiation competent myotubes (Kumar et al., 2004) and a key regulator in the early phase of dedifferentiation. Ectopic expression of an inducible *msx-1* gene combined with growth medium (high serum) stimulation forces cultured mouse myotubes to undergo dedifferentiation (Odelberg et al., 2000). The dedifferentiation process is initiated by down-regulation of factors essential for muscle differentiation. On the first day after induction of Msx1, the muscle differentiation marker MRF4, myogenin and p21 levels were already reduced. MyoD reduction set in on the second day.

Furthermore, on the second day after Msx1 induction the first signs of cleavage could be detected, including stretching of the cells and subsequent cleavage at the end of the myotubes as well as the emergence of progenies from the core of the myotubes. 8.8% of investigated myotubes underwent cleavage and gave rise to multinucleated fragments or even mononucleated offspring. Subsequently, a fraction of the mononucleated offspring started to proliferate. Clonal populations of dedifferentiated cells were further tested to transdifferentiate into different cell lineages. Indeed, it was shown that these clonal populations were competent to redifferentiate into cell types expressing markers of chondrogenesis, adipogenesis, osteogenesis and myogenesis (Odelberg et al., 2000).

3.4.5 Dedifferentiation induced by small molecules

Myoseverin, a trisubstituted purine, was identified by screening a purine library, to have a direct effect on differentiated mouse muscle cells (Rosania et al., 2000). After exposure of myotubes to myoseverin the cells developed cytoplasmatic constrictions between the nuclei. The shape of the myotubes resembled a beads-on-a-string motive. Myoseverin caused a disintegration of the microtubule structure, forming short fragmented microtubules between the nuclei instead of parallel bundles aligned with the long axis of the myotube. Additionally, removal of myoseverin and subsequent culture in proliferation medium yielded BrdU positive cells which points to cell cycle progression (Rosania et al., 2000).
Microarray analysis revealed that incubation of myotubes in myoseverin leads to an altered transcriptional profile compared to untreated control cells. Interestingly, myoseverin did not significantly affect genes involved in cell cycle and muscle specification. Instead, around one half of the transcripts affected by myoseverin are involved in wound healing and tissue repair, comprising genes involved in extracellular matrix remodelling, inflammation, coagulation, signal transduction and cell communication (Rosania et al., 2000).

A triazine compound, which shows structural similarity to myoseverin, also forces mammalian myotubes to cellularise (Duckmanton et al., 2005). Cellularisation was caused again by disruption of the microtubule cytoskeleton. Neither BrdU incorporation nor proliferating progeny could be detected by time-lapse microscopy. Centrioles, which are critical structures for cell

cycle progression are progressively lost during differentiation. In mononucleated cells derived from incubation with the triazine compound, a re-appearance of centrioles in the ratio 2:1 with the nucleus could not be detected. This absence of centrioles in the progeny could possibly be the cause of the absent mitotic activity. In contrast to the experiments performed with myoseverin, as described above, experiments with the triazine compount were carried out on pmi28 cells. The pmi28 cell line, also a mouse myogenic cell line, is more stable in culture and results in a higher proportion of long, narrow and unbranched myotubes. These characteristics seem to be responsible for the higher responsiveness of the pmi28 myotubes to cellularisation for the triazine compound and for myoseverin. Unfortunately, results obtained from incubation with myoseverin concerning cell cycle re-entry could not be repeated on pmi28 cells (Duckmanton et al., 2005).

3.4.6 Implantation and *in vivo* studies of muscle dedifferentiation

Dedifferentiation could be observed by microinjection of cultured newt myotubes with rhodamine-dextran and subsequent transplantation under the wound epidermis of early regenerating limbs (Lo et al., 1993). The tracing dyer could not be transferred between cells. Therefore, it could be excluded that adjacent blastemal cells become stained unintendedly. By harvesting blastemas at different time points after transplantation an increase of labeled mononucleated cells was observed. Thus, it was concluded that the initially labeled myotubes cellularised and further proliferated. After 4-6 weeks the dye disappeared through dilution by proliferation. Nevertheless, the dye was also present in a few newly differentiated chondrocytes (Lo et al., 1993).

The above mentioned result was verified by using a different staining strategy. Insertion of a genetic marker (human placental alkaline phosphatase) into the A1 cell genome the (minor) possibility was excluded that labeled mononucleated cells originated from cytoplasmic transfer of the rhodamine-dextran linage tracer (Kumar et al., 2000). Transplantation of these stained myotubes into the early regenerating tissue gave rise to labeled mononucleated offspring. Furthermore, as an expansion of the above-mentioned experiment, BrdU injection was performed 9 days after transplantation. Analysis after 24 hours revealed that BrdU incorporation was not restricted to the implanted labeled muscle progenitors and blastemal cells. Instead, nuclei in muscle at the distal stump tissue were BrdU labeled as well (Kumar et al., 2000). The observation

of cultured newt muscle cells re-entering the cell cycle after transplantation was consistent with the results described in Section 3.4.2 where cultured A1 myotubes exposed to elevated levels of serum displayed BrdU incorporation.
To learn more about the relationship of cell cycle re-entry and cellularisation (Velloso et al., 2000) studied transplanted myotubes inhibited in cell cycle progression. Cell cycle re-entry was either blocked by X-irradiation or by ectopic expression of p16, an inhibitor of the CDKs 4 and 6 which are essential for G_1/S transition. Although, progression through the cell cycle was blocked mononucleated cell offspring was detected within the regenerate (Velloso et al., 2000).

By using the *Ambystoma mexicanum* (Axolotl) larva which has a thin and translucent skin it is possible to observe single traced cells by Nomarski imaging. (Echeverri et al., 2001) revealed new insight into muscle dedifferentiation by applying this method. After fluorescence labelling of a myofiber *in situ* it was possible to follow this individual syncytial cell. Results verified previous muscle dedifferentiation data exclusively gained on static observations. An interesting finding of this study was that dedifferentiation was only observed if a small cytoplasmic portion was clipped from the end of the muscle cell accompanied by severe tissue injury at the site of surgery. The morphology of the resulting mononucleated cells resembled those of blastemal cells (Echeverri et al., 2001).

3.6 Chromatin

Deoxyribonucleic acid (DNA) is the primary information storage system of life. Besides DNA, there is another system which determines how the primary DNA-information has to be used during different developmental stages in different cells. This second, superordinate system over the DNA, is referred to as the epigenetic system of the chromatin. This epigenetic system comprises DNA methylation and histone proteins with various posttranslational modifications (Thiagalingam et al., 2003). A nucleosome, the smallest unit of chromatin, is composed of 4 different histone proteins (H2A, H2B, H3 and H4) which build up a globular histone octamer wrapped around by roughly two turns of DNA (see Fig. 5). The carboxy terminal parts, which build up a globular structure, are located within the nucleosome whereas the amino terminal tails of the histones are flexible, charged and accessible and thus are subject to posttranscriptional

modifications. Specific amino acid residues of these amino terminal tails can be modified by phosphorylation, acetylation, methylation or ubiquitination (Jenuwein and Allis, 2001).

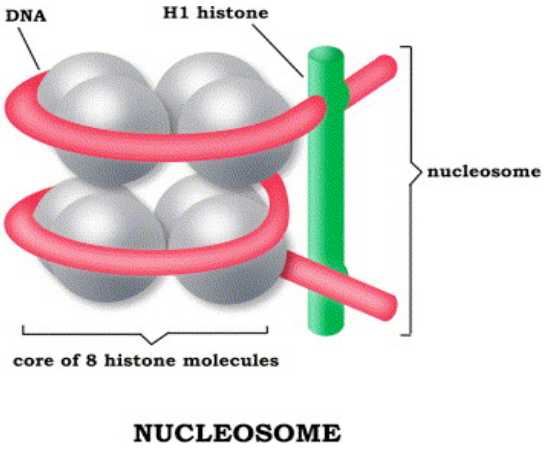

Figure 5. Schematic Illustration of a Nucleosome

The amino terminal tails of the histone proteins (H2A, H2B, H3 and H4) are flexible and protrude from the nucleosome (not visible in this scheme). Therefore, they are able to interact with the DNA and are subject to various posttranslational modifications.

(Figure from (Monneret, 2005))

The importance of epigenetic information storage becomes obvious by the comparison of monozygotic twins. Although these individuals possess identical genetic sequences differences in anthropomorphic characteristics and sensitivity to diseases can be observed. These variations often arise in older twins who have led separate lives or had divergent natural health-medical histories. This becomes evident in differing DNA methylation and histone H3 and H4 acetylation patterns (Fraga et al., 2005).

Whether a gene is transcribed or not depends, from an epigenetic point of view, on the arrangement of chromatin. Chromatin, at the level of transcription, can be at least divided in either euchromatin or heterochromatin (Jenuwein and Allis, 2001). Heterochromatic sections are dense structures which are cytologically visible as heterochromatic foci during interphase. Genes located within euchromatic DNA-sections are transcribed whereas genes inside heterochromatic sections remain inaccessible for transcription factors. This location dependent variation of expression is known as position-effect variegation (PEV) (Jenuwein and Allis, 2001). To alter the status of a gene (on-off state) two groups of proteins exist which have antagonizing effects on chromatin. Factors which positively influence transcription and/or degrade or destabilize heterochromatic marks belong to the class of E(var) proteins (enhancer variegation) whereas factors suppressing transcription belong to the Su(var) (suppressor variegation) family. E(var) protein family members are e. g. histone acetyltransferases (HAT) and factors which increase nucleosomal mobility (e. g. SWI/SNF). Antagonizing factors belonging to the Su(var) group

include proteins such as histone deacetylases (HDACs), protein phosphatases (PPtases) and depending on of their substrate histone methyltransferases (HMTases) (Jenuwein and Allis, 2001; Rea et al., 2000).

Furthermore, the important developmental regulators of the Polycomb (Pc-G) and trithorax (trx-G) groups belong to the PEV. Pc-G belongs to the Su(var) factors whereas trx-G functions to establish euchromation marks like the members of the E(var) group (Jenuwein and Allis, 2001).

Though performing different functions on the chromatin scaffold, members of both groups share highly conserved protein domains. These are the bromo-, chromo- and SET domains, which are conserved from yeast to man (Jenuwein and Allis, 2001; Rea et al., 2000). The bromo domain functions in the recognition of acetylated histone residues, the chromo domain mediated the recognition of methylated histone residues whereas the SET domain has histone methyltransferase (HMTase) activity. The bromo- and chromodomains are the docking domains of histone modifying enzymes. Specificity to a specific location and modified amino acid on the histone tail are the results of recognition of modification marks in a certain context. There are proteins which contain up to six bromodomains. Most likely, this further increases substrate specifity by binding only to groups of acetylated marks that are spaced in a correct manner. Furthermore, this reflects the interdependence of various modification on the same or neighbouring histone tails. These findings seem correlate with the predicted "histone code" hypothesis, that combinations of histone modification marks serve as binding sites for chromatin remodelling complexes (Jenuwein and Allis, 2001).

On the other hand, already established marks have influence on the addition of further marks. For example, histone H3 lysine 9 (H3K9) dimethylation alleviates phosphorylation of histone H3 serine 10 (H3S10) whereas phosphorylated H3S10 and acetylated H3K9 block H3K9 methylation. In contrast, acetylation of histone H3 lysine 14 (H3K14) and H3K9 enhances phosphorylation of H3S10 over the total rate of unmodified substrate *in vitro* (Rea et al., 2000). This illustrates that an already established posttranslational mark influences further deposition of marks on the same histone overhang. This can be either in a synergistic or antagonizing way.

Enzymes exist for each of the different posttranslational histone tail modifications identified so far, which can remove the added mark. Therefore, the whole system seems to be rather plastic. However, surprisingly, epigenetic marks can even be inherited which is now an established observation (Jenuwein and Allis, 2001).

In general, acetylation and methylation at specific loci can be mapped to either activation or repression of gene expression. Acetylation of histone tail residues is generally linked with activation (Strahl and Allis, 2000) whereas methylation can either be activating or repressing, depending on the position of the modification. On the whole, it can be said that single modifications do not seem to be responsible whether transcription of a gene is turned on or off (Strahl and Allis, 2000). Instead, various modifications on histone tails at certain loci are interdependent in triggering or repressing transcription. This combination of different modifications is believed to reflect a "histone code" (Jenuwein and Allis, 2001).

Methylation can either take place at arginine, which is in general an active mark, or at lysine residues, which can be active or repressive marks. Activating methyl lysine marks are H3 lysine 4, 36 and 79 methylation, respectively, whereas methylation of H3 lysine 9, 27 and H4 lysine 20, respectively, marks repression. Lysine can either be mono-, di-, or trimethylated (Klose et al., 2006), presumably reflecting the strength of activation or repression.

3.6.1 Histone H3 lysine 9 (H3K9) methylation

Methylation of H3K9 marks transcriptionally silent chromation regions (Nakayama et al., 2001). Enzymes attaching this mark belong to the originally identified PEV modifier family Su(var)3-9 of Drosophila. These enzymes are conserved from *Schizosaccharomyces pombe* (Clr4) to men (SUV39H1) (Rea et al., 2000).

They share the highly conserved SET domain and chromodomain. The SET domain is bordered by cysteine-rich regions. These regions constitute the catalytic centre, which is sufficient to specifically attach the methyl group to the lysine on position 9 at the amino terminal end of histone H3 *in vitro* (Nakayama et al., 2001; Rea et al., 2000). However, *in vivo* experiments pointed out that the chromodomain is further required to effectively establish the heterochromatic mark (Nakayama et al., 2001).

Upon formation of this methyl mark, heterochromatin protein 1 (HP1) binds via its chromodomain and stabilizes the mark by establishing constitutive heterochromatin, e.g. pericentric regions (Lachner et al., 2001; Nakayama et al., 2001).

Besides its involvement in the origin of constitutive heterochromatin, methylation of lysine 9 on histone H3 is also required in the regulation of facultative heterochromatin, e.g. developmental

genes. However, establishment of facultative heterochromatin seems to be catalysed in a Suv39h1 (mouse homologous to SUV39H1 of humans) independent manner and further proceeds without HP1 binding (Peters et al., 2002).

Enzymes removing this repressive H3K9 mark, either use flavin, such as lysine-specific demethylase 1 (LSD1), or iron and α-ketoglutarate as cofactors within their conserved JumonjiC (JmjC)-domain such as Jmjd1a and Jmjd2c. The latter ones are members of the JmjC-domain-containing histone demethylases (JHDMs) which can reverse all three methylation statuses of lysine residues (Klose et al., 2006).
LSD1 is capable of demethylating mono- and dimethylated lysine residues (Klose et al., 2006). Substrate specificity is achieved in a ligand dependent manner. Therefore, LSD1 can either function as a transcriptional activator (Metzger et al., 2005) or transcriptional repressor (Shi et al., 2004).
Jmjd1a and Jmjd2c are positively regulated by Oct4 and are essential to maintain the self-renewal and pluripotent ("stemness") state of embryonic stem (ES) cells. Jmjd1a specifically demethylates H3K9 dimethylation at the Tcl1 promoter whereas Jmjd2c is required for the active transcription of Nanog by demethylating the H3K9 trimethylated Nanog promotor (Loh et al., 2007).

3.6.2 Trichostation A (TSA)

Histone NH_2-terminal acetylation is catalyzed by histone acetyltransferases (HATs), which attach acetyl-groups, and histone deacetylases (HDACs), which remove this mark. Histone acetylation takes place at definite lysine residues which can overlap with methylation, e.g. H3K9 (see above). Hyperacetylation at a certain locus is commonly associated with active transcription. On the other hand, transcriptionally silent heterochromatin is usually marked by hypoacetylation. The degree of acetylation is regulated via shifts in the equilibrium of acetylation and deacetylation. Thus, HDAC inhibition results primarily in an increase of histone acetylation (Monneret, 2005; Yoshida et al., 1990).
There are 3 different groups of HDACs. The classification is based on similarity to the forms initially identified in yeast. Class 1 HDACs share homology to the Rpd3 protein in yeast and

comprises HADC 1, 2, 3 and 8. They are located within the nucleus. Class 2 HDACs (HDAC 4, 5, 6, 7, 9 and 10) are similar to the yeast Hda1 protein. They are located in the cytoplasm and nucleus. The third class of HDACs resembles the Sir2 protein from yeast which are NAD-dependent enzymes and thus structurally different from class 1 and class 2 (Thiagalingam et al., 2003).

TSA (see Fig. 6) was isolated from Streptomyces hygroscopicus and originally identified as an antifungal antibiotic. It is a potent inhibitor of class 1 and class 2 HDACs in a noncompetitive way even at nanomolar concentrations (Kyrylenko et al., 2003; Yoshida et al., 1990). It interacts with the active centre, which is conserved in class 1 and class 2 HDACs (Finnin et al., 1999).
The consequences of HDAC inhibition are heterogeneous and, as far as they are known, range from cell cycle arrest and differentiation (Yoshida et al., 1995), activation of host immune response and inhibition of tumor angiogenesis (Monneret, 2005), to caspase 3 activation promoting apoptosis (Salminen et al., 1998). Therefore, one possible promising application of HDAC inhibitors would be cancer therapy (Johnstone, 2002).

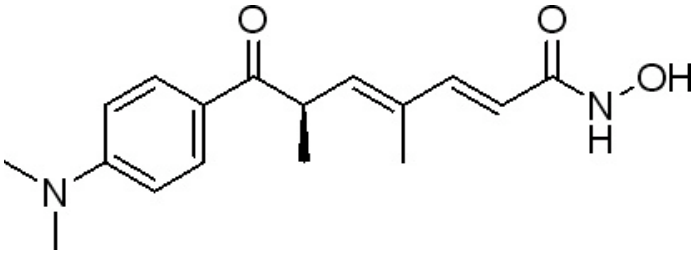

Figure 6. Molecular Structure of TSA

(Figure from www. Sigmaaldrich.com)

3.7 Specific aim of the study

The specific aims of this study were twofold:

First, to examine chromatin modifications on histological sections of regenerating tissue of the newt aiming at the identification of differences in histone methylation patterns between normal and regenerating tissues.
Tissue from phase I of the limb regeneration process (see Section 3.2.1) was used because we wanted to investigate changes in chromatin-modifications in blastema progenitors. In particular, the focus was on the process of dedifferentiation of differentiated tissue.
Based on differences in chromatin methylation patterns reactivated cells should be distinguished from limb tissue cells. Methylation at specific residues at the NH_2-terminal domain of histone H3 characterise transcriptionally silenced domains (see above). An indication of dedifferentiating cells should be gained by comparing tissue sections of different time points of the initial stages of limb regeneration. As it is hypothesised that the loss of methylation in a given cell/tissue is a sign of re-activation and further dedifferentiation, special attention was paid to the loss of methylation marks.

Second, to assess how changes in chromatin modifications may influence skeletal muscle cell plasticity. In particular, the effect of histone deacetylase (HDAC) inhibitor Trichostatin A (TSA) on the plasticity of newt myotubes (A1) and murine myotubes (C2C12) was examined. Experiments were performed to gain insight to the molecular mechanisms underlying dedifferentiation.
However, the triggers for the dedifferentiation process are known (Echeverri et al., 2001; McGann et al., 2001; Odelberg et al., 2000) knowledge of the underlying mechanism is almost absent.
Therefore, we tried to define the role of histone deacetylases during the dedifferentiation process. Histone deacetylases are regulatory enzymes whose substrates are located in the nucleus and cytoplasm depending on the HDAC.
Previous experiments in our laboratory already indicated that serum treatment induced cell cycle re-entry of cultured newt myotubes which is accompanied by histone H4 lysine 12 acetylation.

This result triggered our investigation of the direct increase of elevated acetylation levels in detail.

4. Results

Preliminary analyses were carried out to uncover possible changes in the state of chromatin of normal and early regenerative tissue, respectively.
Furthermore, to test whether histone deacetylation is involved in the process of myogenic dedifferentiation and to learn more about the plasticity of the differentiated state, the effects of TSA on differentiated myotubes were analysed. Of particular interest was the ability of TSA to induce the fragmentation of multinucleate myotubes to progeny with a reduced number of nuclei or with only one nucleus.

4.1 Differences in histone modifications between normal limb tissue and regenerating stump tissue in situ

Antibodies against histone H3 lysine 9 (H3K9) methylation patterns were used to examine chromatin alterations during the initial steps of regeneration.
For this purpose, tissue sections of normal limb and regenerating stump tissue of day 3 and 10 post amputation (p.a.) (see Material and Methods) were stained with antibodies against histone H3K9 di-methylation, histone H3K9 tri-methylation (see Introduction) and DAPI.
Afterwards, the cells were screened for differences in the methylation state in relation to their anatomical location. Antibody staining in combination with DAPI staining showed that the antibodies specifically stained the nucleus, as had been expected. This was important, as there have been no reports of these antibodies working in newts, so far.

In addition to the specific binding in the nucleus, the antibody against tri-methylated histone H3K9 produced a strong background signal. This phenomenon was observed on normal limb tissue sections and sections taken three and ten days after amputation, mostly in muscle cells and extracellular structures (see Fig. 7). Generally, signal intensity of this antibody was weaker than the one seen with the antibody against histone H3K9 di-methylation.

In normal limb tissue sections both antibodies bound uniformly throughout the whole tissue section. Fig. 7 shows that all nuclei stained with DAPI were also positive for histone H3K9 di-methylation and tri-methylation, respectively. This is consistent with the expected result under physiological condition without trauma.

Furthermore, throughout the sections analysed, in many nuclei a zone could be observed where the staining signal was more intense. This effect was not observed in all nuclei, presumably due to how the cells were sliced (see Fig. 7).

Moreover, the intensive nuclear staining zone was rare with the antibody against tri-methylated histone H3K9 as compared to the antibody against di-methylated histone H3K9.

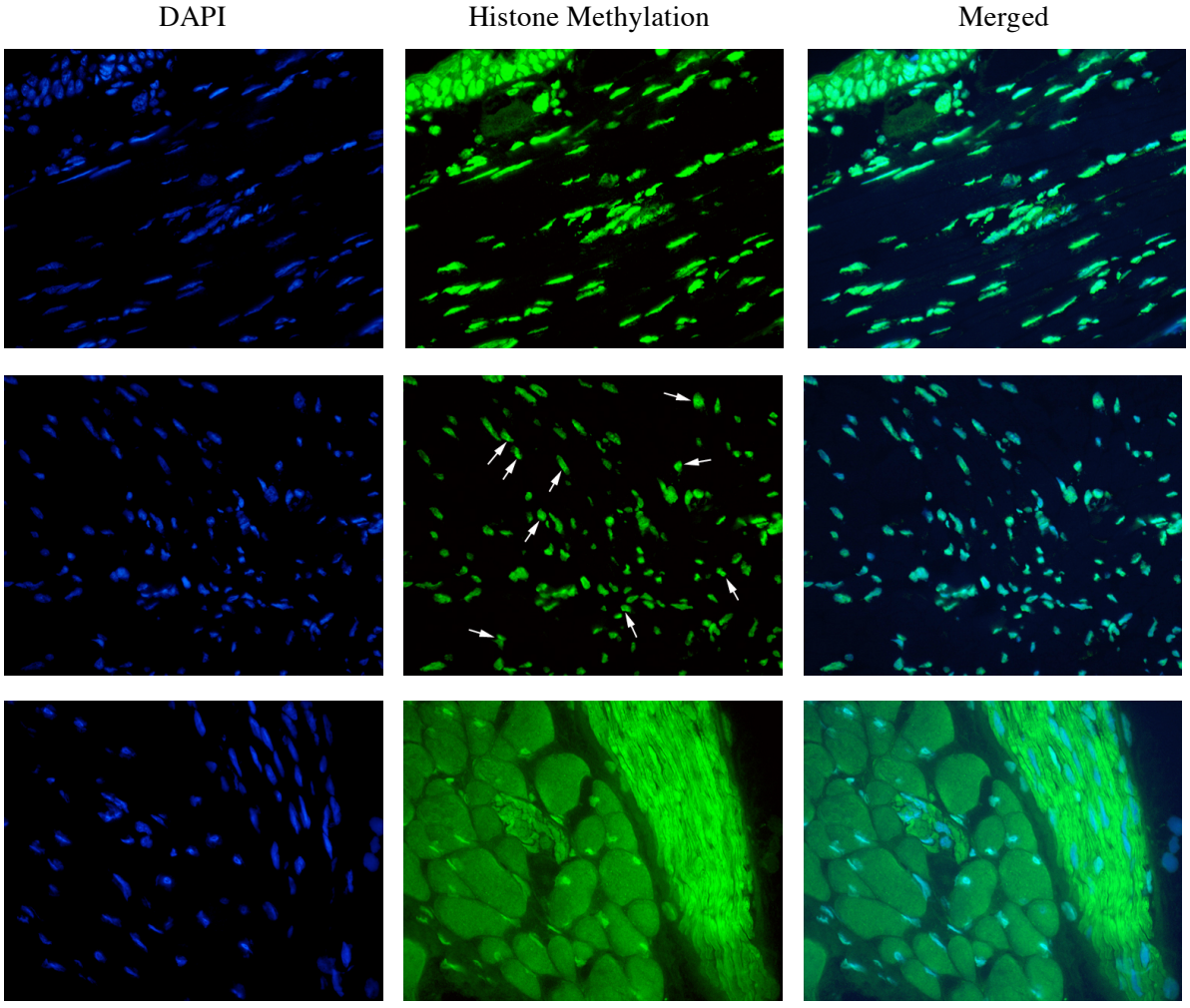

Figure 7. Uniform Histone H3K9 Methylation in Non Regenerating Newt Limb

Upper row: Section from normal newt limb tissue stained against di-methlyation of histone H3K9. As can be seen, there is no obvious difference between single cells throughout the tissue. Except, in the upper left corner of the images where a portion of the epidermal layer can be seen. The epidermis is generally very intensively stained.
Middle row: Zones within the nuclei with more intensive staining compared to the surrounding chromatin (indicated by arrows)
Bottom row: The unspecific binding of the antibody against histone H3K9 tri-methylation. As can be assumed by staining pattern the structures are mainly to muscle tissue and extracellular matrix.

Analysis of the di-methylation state of tissue sections 3 and 10 days p.a. revealed a change in the signal intensity and staining pattern of this antibody.
3 days p.a., the staining intensity was comparable to normal limb sections. An exception was a zone beneath the wound epidermis, in the very early regenerative tissue, where DAPI and histone H3K9 di-methylation signals were practically absent.
However, in tissue sections 10 days p.a. a visible change of staining pattern occurred. Importantly, signal intensity in the blastemal cells was noticeably reduced (see Fig. 8). Moreover, a very dominant region of the dermis was detected directly beneath the epidermal layer at the blastema-tissue boundary. However, it was not possible to further characterize these cells at that time. Furthermore, the cells in the centre of the regenerate beneath the wound epidermis were very weakly stained.
Tissue proximal to the amputation site appeared unchanged compared to normal tissue.

In contrast to the staining performed against histone H3K9 di-methylation, staining intensity against histone H3K9 tri-methylation changed already on day 3 p.a.. In this case, staining intensity on day 3 p.a. against histone H3K9 tri-methylated was already comparable to that observed in tissue sections 10 days p.a. stained for histone H3K9 di-methylation. Again, the region beneath the epidermal layer was the most dominant in terms of a reduction of signal intensity besides the blastemal cells. Only very faint staining could be observed in this zone (see Table 1).
After day 3 p.a. staining intensity against histone H3 lysine 9 tri-methylation remained constant up to day 10 p.a..
As before, proximal to the amputation plane staining appeared similarly as has been detected in normal limb tissue sections.

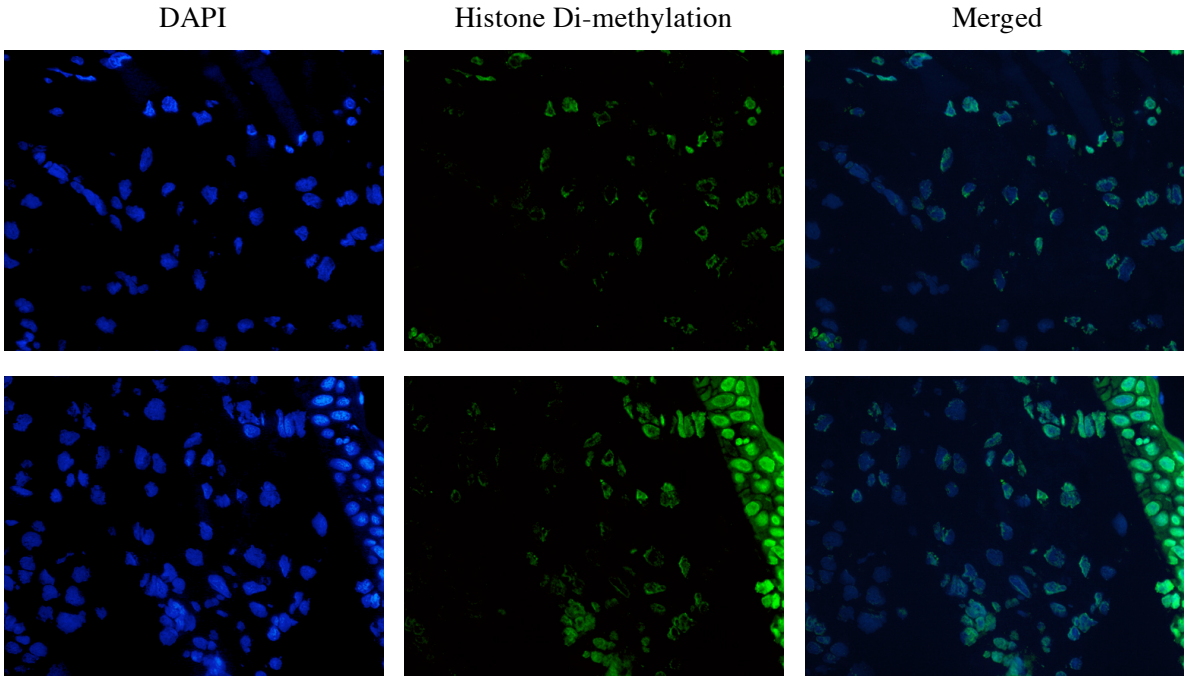

Figure 8. Change in Histone H3K9 Di-Methylation 10 Days Post Amputation

Upper row: Blastemal cells. Compared to normal limb tissue an obvious reduction of histone H3K9 di-methylation can be detected.

Bottom row: Image of the blastema-tissue boundary. Epidermal cells (on the right) seem to be unaffected though cells beneath the epidermal layer are slightly reduced in histone H3K9 di-methylation compared to normal limb tissue sections.

In the epidermal layer no change could be observed in the staining patterns of either of the two antibodies at all three time points.

	Epidermis H3K9dM / H3K9tM	Dermis (at amputation site) H3K9dM / H3K9tM	Blastema H3K9dM / H3K9tM
Normal limb tissue	3 / 3	3 / 2	N / A
3 days post-amputation tissue	3 / 3	2.5 / 1	0.5 / 0.5
10 days post-amputation tissue	3 / 3	1 / 0.5	0.5 / 0.5

Table 1: Categorization of Staining Intensities at Distinct Regions

0 to 3 represents the staining intensities observed where 0 indicate no staining and 3 the strongest.

4.2 Trichostatin A (TSA) triggers murine myotubes to dedifferentiate

To examine the effect of TSA on dedifferentiation, C2C12 cells were grown to confluence and induced to differentiate into myotubes. Myotubes are terminally differentiated by definition. This means that they are multinucleated and express markers of terminal differentiation, for example myosin heavy chain (MHC) and muscle creatine kinase (MCK). Furthermore, they are also refractory to growth factor stimulation.
96 hours after induction to differentiate, myotubes were picked (see Materials and Methods) in order to obtain samples without mononucleated cells. Thus, preexisting contamination with mononucleated cells was reduced to a minimum, which was essential as the mononucleated offspring generated by TSA-treatment were the subjects of interest.

In order to determine the conditions under which most myotubes formed progeny with fewer nuclei or with a single nucleus, different incubation times with variable concentrations of TSA were tested.
At first, a concentration of 50 ng/ml TSA in conditioned differentiation medium (see Section 6.1.6) was applied for 8 hours. Afterwards, the TSA action was terminated by changing to fresh conditioned differentiation medium. The wells were fixed in intervals of eight hours, such that the first well was fixed immediately after changing to fresh medium, and the last well 32 hours after the termination of TSA treatment.

The same procedure was repeated with constant TSA concentration but different incubation times. TSA was added for 16, 24, and 32 hours, respectively. Rinsing of the TSA containing medium and subsequent incubation in conditioned differentiation medium for 0, 8, 16, 24 and 32 hours before fixations were performed as described above (see Fig. 9).

These treatments did not yield significant numbers of myotube fragmentation. Most likely the initial TSA concentration was too high, since the number of myotubes decreased rapidly due to cell death the longer the treatment lasted. Furthermore, a significant decrease in MHC signal intensity was observed with increasing incubations.

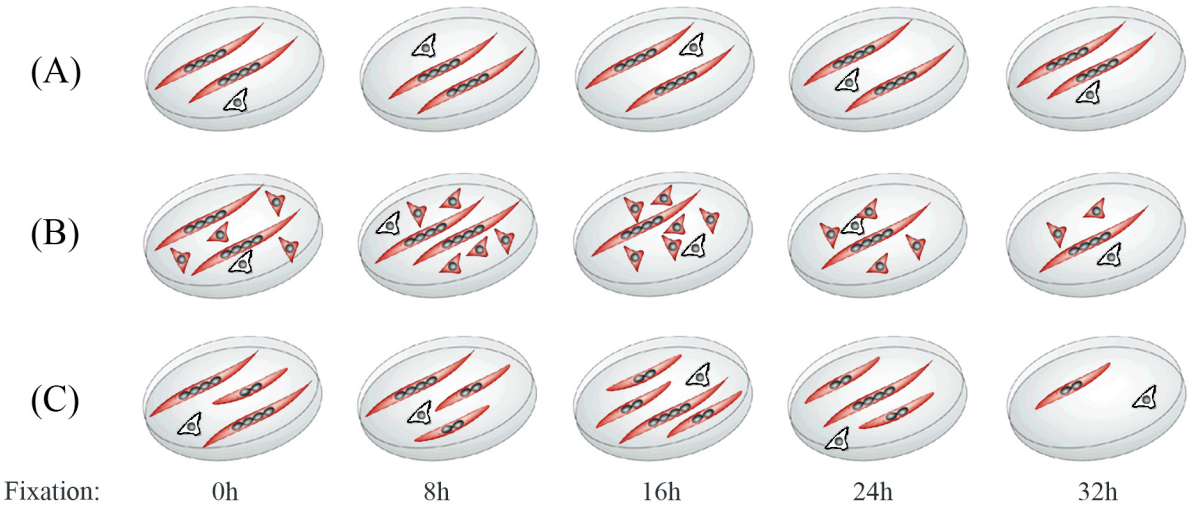

Figure 9. Schematic Illustration of Experimental Procedure

Experimental settings, as indicated in the scheme and described in Material and Methods, were always the same. The initial number of myotubes before the experiments was around 50 per well. Time points in the last row indicate the period of incubation in conditioned differentiation medium between TSA treatment and fixation.

Myotubes are indicated by elongated cells containing 4 nuclei. Mononucleated cells have triangular shape in this scheme. Fragmentation offspring are indicated by longish cells containing two nuclei. Red indicates MHC-positive cells, white indicates MHC-negative cells.

(A) Control wells were not incubated with TSA but were otherwise treated similarly. Residing contamination with mononucleated MHC-negative cells is indicated in the scheme while the background of mononucleated MHC-positive cells was omitted.

(B) Expected result: Cellularisation is induced by TSA treatment. As a result, mononucleated MHC-positive cells besides syncytial myotubes can be observed. After longer periods of time average cell number is reduced by cell death.

(C) Actual result: Myotube fragmentation into progeny containing less nuclei was induced by TSA. Best results were obtained by fixation 16 hours after TSA treatment. Again, a considerable number of cells died after longer periods of time. Mononucleated MHC-positive cells above background level could not be observed.

Therefore, TSA concentration was decreased in subsequent experiments. Fixation was performed immediately after TSA incubation. As the presence of MHC served as a marker to identify mononucleate cells derived from multinucleated myotubes, it was very important to monitor MHC levels throughout the experiment.

Results were analysed after fixation and staining against MHC. DAPI was used to identify nuclei (see Materials & Methods). The analysis was focused on morphological differences between the TSA incubated myotubes and myotubes in the corresponding control well. Additionally, the number of nuclei per cell should have served as another indicator for dedifferentation.
MHC-positive cells containing one nucleus could be observed in TSA treated as well as in control wells without TSA. As can be seen in Table 2, there was no difference in the frequency of appearance of these particular cells. Since the number of generated mononucleated MHC-positive progeny did not allow us to clearly attribute an effect of TSH on myotubes, we then set 5 nuclei/cell as an arbitrary limit to monitor possible dedifferentiation effects. Even with this criterion, a TSA concentration of 5 ng/ml did not provoke detectable differences (see below).

Since our original aim was to identify MHC-positive mononucleated cells, we examined myotubes incubated with varying concentrations of TSA for varying lengths of time. We observed that TSA concentrations of 20 ng/ml yielded significantly reduced nuclei-numbers in fragmented myotube-progeny and also caused dramatic changes in morphological appearance. However, under these conditions, cells died rapidly.
Therefore we used lower TSA concentrations for further experiments. Although reduction of nuclei number in myotube fragments was not significant at 5 ng/ml, morphologically, these cells were clearly distinguishable from controls, indicating that same fragmentation was already occurring (see Fig. 10). Under these conditions, the cells remained viable and could be readily analysed.
As can be seen in Fig. 10, cells without TSA treatment were branched and contained a considerable number of nuclei. In contrast, the cells after incubation with 5 ng/ml TSA were noticeably smaller and unbranched. This was particularly apparent in myotubes in the centre of these wells, where the cells usually accumulate after purification.

The significant morphological difference to the control well and the high residual cell number (see Table 2) were the decisive factors to continue with 5 ng/ml TSA.

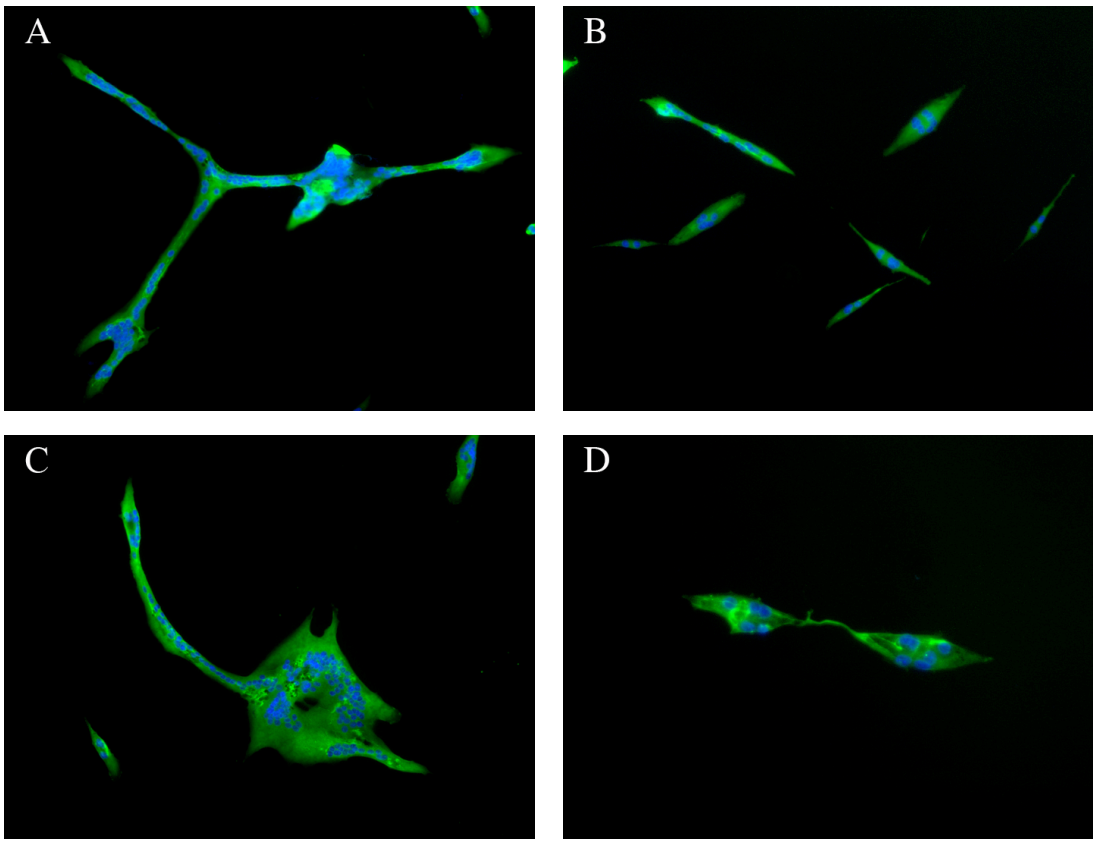

Figure 10. Effect of TSA on Cells in Wells from the Same Plate

(A&C) Control without TSA treatment.
(B&D) Myotubes after exposure to 5 ng/ml TSA for 48 hours.

A clear difference between the TSA treated and the untreated control myotubes can be seen. Control myotubes had several dozen of nuclei and a branched morphology. Big myotubes as can be seen in the control well (A, C) could not be found in the TSA treated well.
The bottom picture on the right (D) shows two parts of a myotube still connected through a thin cytoplasmatic bridge (20x magnification).
Blue indicates DAPI staining and green represents staining against myosin heavy chain (MHC).

Photos were taken from the centres of the wells because the cells tended to accumulate there. Huge myotubes containing several dozens of nuclei could be detected in the untreated control wells, whereas the cells were remarkably smaller and contained less nuclei after TSA treatment.

	Control							TSA							
	Total	+ MHC					- MHC	ng/ml	Total	+ MHC					- MHC
		Multi	Mono	≤ 3 N	4 N	5 N	Multi/ Mono			Multi	Mono	≤ 3N	4 N	5 N	Multi/ Mono
C2C12 / 48h	46 100%	10 21.6%	3 6.4%	17 37%	6 13%	5 11%	0/5 0/11%	5	69 100%	22 31.9%	2 2.9%	23 33.3%	8 11.6%	6 8.7%	0/8 0/11.6%
								10	37 100%	12 32.4%	1 2.7%	11 29.7%	2 5.4%	3 8.1%	0/8 0/21.6%
								20	22 100%	7 31.8%	1 4.5%	6 27.3%	3 13.6%	2 9.1%	0/3 0/13.6%
C2C12 / 72h	111 100%	28 25.2%	4 3.6%	19 17.1%	9 8.1%	6 5.4%	0/45 0/40.6%	5	74 100%	22 29.7%	0	22 29.7%	11 14.9%	5 6.8%	0/14 0/18.9%
								10	47 100%	10 21.3%	0	11 23.4%	9 19.1%	2 4.3%	0/15 0/31.9%
								20	14 100%	2 14.3%	0	9 64.3%	1 7.1%	0	0/2 0/14.3%
A1/24h	42 100%	23 54.7%	1 2.4%	11 26.2%	n.c.	n.c.	0/7 0/16.7%	5	43 100%	16 37.2%	2 4.7%	11 25.6%	n.c.	n.c.	0/14 0/32.6%
A1/48h	28 100%	10 35.7%	3 10.7%	7 25%	n.c.	n.c.	0/8 0/28.6%	5	38 100%	22 57.9%	2 5.3%	7 18.4%	n.c.	n.c.	3/4 7.9%/10.5%
A1/72h	16 100%	8 50%	1 6.25%	4 25%	n.c.	n.c.	0/3 0/18.75%	5	33 100%	20 60.6%	3 9.1%	6 18.2%	n.c.	n.c.	0/4 0/12.1%

Table 2. Cell Numbers in Control and TSA-Incubated Wells after Fixation

As can be seen, with increasing concentrations and incubation times of TSA the overall amount of cells decreases continuously. All these experiments were carried out in 24 well plates. Purified cells were kept in 1 ml conditioned proliferation medium and TSA or without TSA, which served as negative control.
n.c.: not counted

Negative controls were performed for each experiment. For that purpose, cells were picked from the same pool of differentiated myotubes into wells of a 24-well plate. Then the cells were treated with variable concentrations of TSA for the same period of time. The cells in the corresponding control wells without TSA were kept in conditional differentiation medium for the same time. Subsequently, the cells were all fixed simultaneously and subjected to further analysis.

4.3 Imaging fragmentation of single mammalian myotubes by time-lapse microscopy

To find out more about the morphological changes during myotube fragmentation, time-lapse microscopy was applied.
Myotubes were picked as described in Material and Methods (see Section 6.1.6). The purified myotubes were cultured in a 3 cm dish to fit the requirements of the time-lapse microscopy equipment.

A motorized stage enabled a higher throughput of image-taking (up to 30 predetermined fields at each chosen time point). The effects induced by TSA were usually examined for four days during which pictures were taken every hour. During this period the C2C12 myotubes were maintained in differentiation medium containing 5 ng/ml TSA (see Section 4.2; except in initial experiments cells were kept in L15 medium as mentioned in Section 6.5.2). In contrast to the experiments described in section 4.2 TSA was not removed from cells after a certain period but the cells were incubated with TSA-containing medium for the whole procedure of time-lapse microscopy. This was necessary as the culture dish must not be moved during the time-lapse procedure in order to avoid relocation of the predetermined positions.

Figure 11 shows one example of a myotube that fragmentates into two smaller progeny. The first signs of fragmentation became evident around 12 hours after induction with TSA. The cleavage process continued for the next two hours and resulted in two completely separated smaller multinucleated myotubes. The two progeny remained quiescent for three hours. Then, one of the cells died while the second daughter cell died two hours later.
In all time-lapse experiments done during this study none of the observed myotube cleavages resulted in mononucleated progeny nor was there any evidence that one of the cleavage fragments started proliferating again.

A total of 90 movies from 3 independent experiments were assembled and analyzed, always yielding the following results:

First, the myotubes elongated after induction with TSA.
Second, the nuclei moved to opposite poles of the elongated myotube.
Subsequently, disruption of the myotube occurred close to the centre. Unfortunately, all cells died after the disruption.
In most cases the sequence of events was the same and only the time intervals of and between the different stages varied.

Only a few myotubes did not react to the TSA treatment in the above-mentioned way. They stayed in a more globular shape and died at a later time point, approximately after three days.

Results gained by time-lapse microscopy confirmed the decision (see Section 4.2) to continue experiments with a concentration of 5 ng/ml TSA. Fragmentation as has been described in Fig. 11 could be observed frequently but never yielded progeny containing five or less nuclei.

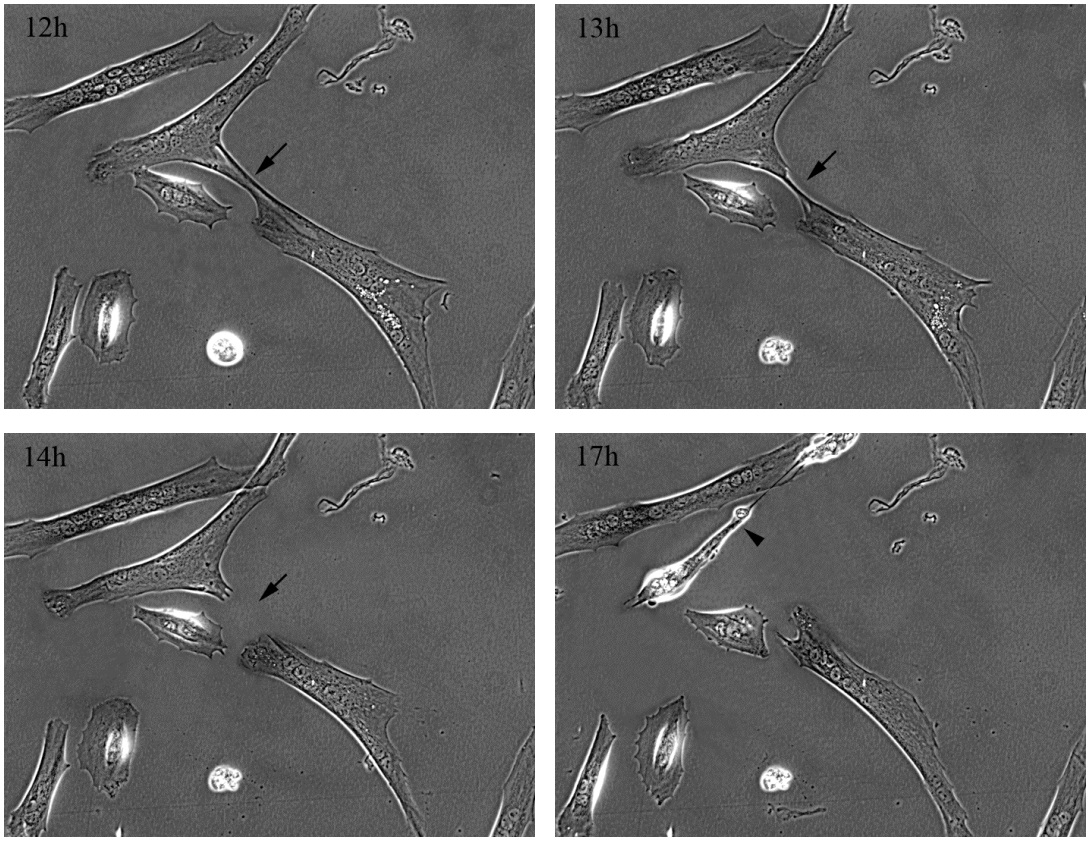

Figure 11. Time-lapse Microscopy of Fragmentation of a Murine Myotube

Single frame images from a myotube exposed to 5 ng/ml TSA. The arrows indicate the connecting cytoplasmatic bridge. Cleavage yielded progeny that were not mononucleate but had fewer nuclei than the original cell. Budding of a singular nucleus from the syncytium could never be observed. After the accomplishment of cleavage, the offspring remained quiescent for at least three hours until first signs of cell death could be observed (arrowhead).

4.3 BrdU incorporation assay to evaluate if TSA treatment causes cell cycle re-entry in C2C12 myotubes

Besides cellularisation, cell cycle re-entry is another criterion of myogenic dedifferentiation (Duckmanton et al., 2005).

To address this question, purified C2C12 myotubes (see Materials and Methods) were treated with TSA. After an incubation period of 24h the differentiation medium containing TSA was removed followed by incubation in conditioned proliferation medium (high serum medium)

containing BrdU. BrdU is a nucleotide analogue that incorporates into the DNA of cells undergoing S-phase. High serum medium serves as a growth factor stimulating environment, whereas the conditioned differentiation medium used in the previously described experiments served as a differentiation stimulating environment. Although preliminary experiments showed that conditioned differentiation medium provides a better environment for isolated myotubes compared to conditioned proliferation medium, in this case it was essential to stimulate cell cycle re-entry of the myotubes after TSA treatment to test whether the produced progeny can proliferate.

In order to test if cell cycle re-entry and DNA-replication occur, cells were assayed for BrdU incorporation into newly synthesized DNA via immunocytochemistry.

No BrdU incorporation could be detected independent of the length of incubation in proliferation medium (see Section 6.1.8), indicating that no S-phase re-entry occurred.

4.4 Cell death induced by TSA treatment

TSA is a proapoptotic drug and causes programmed cell death (Johnstone, 2002). For this study it was important to investigate whether the myotubes really fragmentized due to the influence of TSA.

To investigate whether cell death pathways were activated in C2C12 myotubes in the presence of TSA, an antibody against the active form of caspase 3 was used. Caspase 3 is known to be one of the major regulators of cell death.

For this purpose the same experimental procedure was applied as has been described in Section 4.2. Accordingly, the cells were incubated with 5 ng/ml TSA for 48 hours.

As a positive control for this experiment, cells were incubated in serum-free medium containing 0.5 mM Staurosporine (see Section 6.1.9). Positive control results indicated that active caspase 3 was localised next to the nucleus in apoptotic cells and to some extent overlapped with nuclear staining.

Unfortunately, no conclusive results could be obtained from these experiments. To date, new experiments are in progress to investigate possible involvement of TSA-induced apoptotic pathways in dedifferentiation.

4.5 Inductive effects of TSA on A1 myotube fragmentation

Upon injection into a regenerating stump, cultured A1 myotubes undergo cellularisation and contribute to the mesenchymal cell mass, also referred to as blastema (Lo et al., 1993).

In order to test the ability of A1 myotubes to cellularise in vitro, A1 myotubes were isolated (see Material and Methods) and incubated with TSA. Incubation periods of 24, 48 and 72 hours, respectively, were chosen while the concentration of 5 ng/ml TSA remained constant.

As has been described in Section 4.2, fragmentation of murine myotubes could be observed after incubations in 5 ng/ml TSA for 48 hours. Similar effects were expected in newt myotubes, with the general difference that responses to exogenous signals seem to be delayed in newt cells. For this reason, the longer incubation time of 72 hours was applied.

The effects of TSA on A1 myotubes were similar but not identical to those observed on murine C2C12 cells. Fragmentation did occur but was not as frequent as in murine myotubes, whereas the rate of cell death was increased. The residual cells were examined for MHC and number of nuclei. Again, no significant amount of mononucleated cells above background level could be detected (see Table 2).

Moreover, morphological changes could be detected in A1 myotubes in response to TSA. The cells elongated and migration of the nuclei into the newly formed extensions took place. However, the final step of fragmentation, budding, did not occur (see Fig. 12). For this reason, the morphological difference between TSA-incubated newt myotube cultures and the cells of the untreated control wells was not very conspicuous.

Accordingly, the results gained of TSA-induced A1 myotubes significantly differ from the results obtained of murine myotubes as described in Section 4.2.

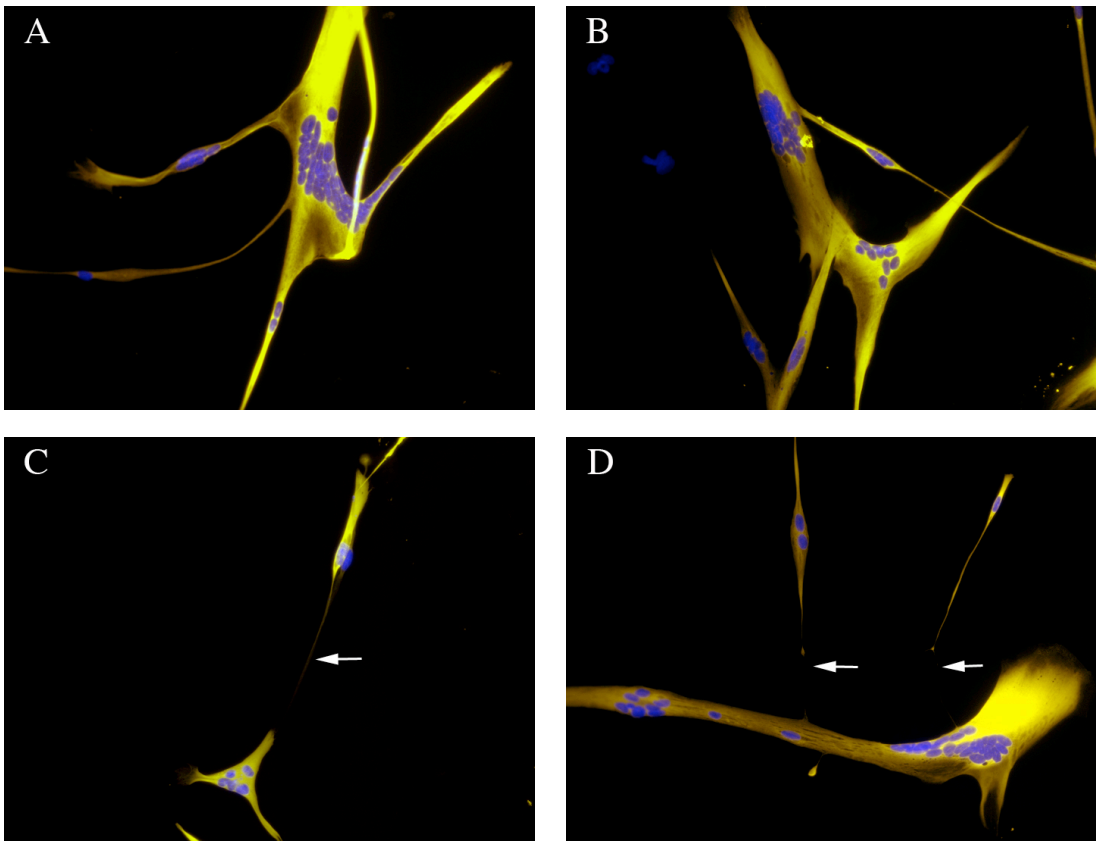

Figure 12. Effect of 5 ng/ml TSA for 48 Hours on A1 Myotubes

(A&C) Control well
(B&D) TSA-incubated cells

Panels A&B show representative myotubes from the centre of control and TSA-treated well, respectively. In contrast to C2C12 myotubes (see Fig. 10), there is no obvious difference between them.
Panels C&D show myotubes where nuclei migrated into cytoplasmatic extensions. These extensions were still connected to the cells (indicated by arrows). This migration of nuclei was detected in control wells as well as in TSA treated wells.
Blue indicates DAPI staining, yellow represents staining against myosin heavy chain (MHC).

4.6 Microinjections of non-isolated A1 myotubes and subsequent incubation with TSA

In order to circumvent the stress imposed on the cells during purification, a new method was applied (Morrison et al., 2007).

Thereby, the differentiated cells were traced expressing various molecules as described in Section 6.3. The cells were microinjected with high molecular weight dextran or plasmids carrying the red fluorescence protein (RFP) as a reporter gene or the fusion protein H2B-YFP (histone 2B-yellow fluorescence protein). Refer to Section 6.3.3 for detailed experimental settings. This method has not been applied to newt myotubes before. The advantage over previous experimental settings was that the differentiated cells did not need to go through an extra purification step, which is challenging for their survival.

As expected, the H2B-YFP stained the nuclei whereas dextran and the RFP stained the cytoplasm of the myotubes.

With the applied microscopic analysis it was not possible to examine if all the injected cells were traced. Nevertheless, the observed traced cells were sufficient to determine the effect of TSA on the differentiated non-isolated myotubes.

Up to 150 ng/ml TSA was used in this experiment (see Material and Methods). As muscle cells exhibit contact inhibition when growing too dense (Tanaka et al., 1997) these higher TSA concentrations were used in order to countervail this phenomenon.

However, despite the high TSA concentrations no fragmentation/dedifferentiation could be observed. All examined positively stained myotubes (surrounded by unstained myotubes or myoblasts) remained in their natural conformation or changed to a more globular shape with increasing TSA concentrations. None of the TSA concentrations used induced an event that could be interpreted as budding of smaller cell progeny, and not even the formation of cytoplasmatic extensions could be observed.

5. Discussion

5.1 Histone H3 lysine 9 (H3K9) methylation and regeneration

So far, all results gained in studies on limb regeneration predict progeny of differentiated cells close to the amputation plane to form a mesenchymal cell mass referred to as blastema. It seems that a dedifferentiation process yields uncommitted cell offspring that possesses stem cell-like properties. To date, it is a matter of debate which progenitors and in which location within the stump tissue contribute to the dedifferentiation process. Dermal fibroblasts (Gardiner et al., 1986) might be involved as well as muscle cells, chondrocytes, Schwann (Ferretti and Brockes, 1991) cells or satellite cells (Morrison et al., 2006). Neither of these cell types can be excluded while on the other hand it is not proven if they are involved in the process at all. To gather more information concerning which cells in which location within the stump tissue participate in the dedifferentiation process, studies have been executed on the basis of chromatin modifications. Chromatin modifications can lead to an altered gene expression, which is required for a cell to acquire new properties (Jenuwein and Allis, 2001). Furthermore, altered gene expression is a prerequisite of dedifferentiation. The emphasis in the initial phase of this experiment was on the detection of a general alteration in histone modification in the stump tissue without focusing on a specific cell type. The intention of the study was to identify progenitors of the blastema.
For a better detection of all cell types, tissue sections of 6 µm thickness were chosen, as they proved to be the most suitable for this purpose in independent studies in our lab.
Cultured satellite cells contribute to the regenerate when injected intramuscularly before amputation (Morrison et al., 2006). Therefore, we wanted to investigate whether satellite cells are subjects of chromatin alterations during the initial steps of regeneration as well.

Generally, histone H3K9 methylation is associated with transcriptional repression (Nakayama et al., 2001). This study was partly aimed at the identification of cells that contribute to regenerating tissue on the basis of histone H3K9 de-methylation. H3K9 de-methylation is usually associated with relaxed chromatin allowing access of transcription factors (Klose et al., 2006; Loh et al., 2007). The de-methylated state, i.e. the loss of methylation was to be detected by specific

antibodies comparing tissue sections of regenerating and normal limb tissue. A reduction of histone H3K9 tri-methylation, usually a sign of very dense chromatin, could already be detected 3 days after limb amputation (see Table 1). Furthermore, a loss of histone H3K9 di-methylation, correlating with a less tight packing of chromatin as observed in tri-methylation, became apparent 10 days after tissue removal (see Fig. 8). A possible explanation for the observed phenomenon could be that reversion of tight repression in terms of histone H3K9 tri-methylation was followed by reversion of the chromatin attachments at specific loci at later time point in regeneration.

The most apparent differences between tissue sections 3 and 10 days post amputation and normal limb tissue sections can be assigned to cells next to the amputation plane and to the subepidermal region at the blastema-stump-boundary. So far, the obtained results represent the proposed niches for progenitor cells in general (see above). At this point of the project, however, no accurate specifications of the involved cell types can be made. However, the results of this diploma work demonstrate that tissue sections from early blastema stained for histone H3K9 tri- and di-methylation showed very weak staining. This could indicate a reversion to the uncommitted state.

An interesting observation was made within observed nuclei. On normal limb tissue- and on 3-days-post-amputation tissue sections stained against histone H3K9 di-methylation a zone within the nuclei appeared brighter compared to the surrounding chromatin (see Fig. 7). Possibly, these bright chromatin zones represent a heterochromatic part containing genes for regeneration. This hypothesis is consistent with a recent report of Murakami et al., (2007). Accordingly, regeneration-specific genes could be mapped to the short arm of chromosome 7. At the later time point of 10 days post amputation where a noticeable loss of staining intensity was observed could indicate the transcriptional activation of the involved genes. The zone possibly corresponds to the region of the short arm of chromosome 7 (Murakami et al., 2007).

The same staining technique using the same antibodies for histone H3K9 tri- and di-methylation, respectively, yielded no results when applied to wound epidermal cells. The signal intensity resembled normal limb tissue in tissue sections taken 3 days as well as 10 days after amputation. The reason for this is still unclear. Post-amputational wound closure is mediated by rapid movement of epidermal cells from the margin of the injury over the wound. 9 hours after limb

tissue truncation the wound surface is closed by the migrated epidermal cells. During cell migration, a transition of heterochromatin nuclei (according to the situation before trauma) to nuclei containing more euchromatin can be observed in the involved epidermal cells (Repesh and Oberpriller, 1980). Furthermore, this newly established epidermis, referred to as wound epidermis, is thought to be a signalling centre for the consecutive regeneration process.

One explanation for our negative staining result could be that 3 days post amputation (which was the earliest time point of taking tissue sections) the chromatin alterations in epidermal cell nuclei are already reverted into their pre-amputation configuration. As wound closure by epidermal cells is already completed 13 hours after limb amputation (Repesh and Oberpriller, 1978) this seems to be not only possible but reasonable.

Another reason might be a different regulation of chromatin alterations in epidermal cells. Histone acetylation instead of histone methylation could be used as a control mechanism for the accessibility of regulatory gene sequences.

To date, the mechanisms that alter epidermal chromatin conformation remain unclear.

5.2 Trichostatin A causes myotube fragmentation

Stimulation of terminally differentiated newt myotubes with 12% FCS containing medium leads to cell cycle re-entry (Tanaka et al., 1997) and associated acteylation of histone H4 lysine 12 (H4K12) (Simon A., unpublished data) (see Fig. 13). Therefore, experiments in our group (Lööf S., unpublished data) were carried out to examine if the inhibition of histone deacetylases (HDAC) leads to cell cycle re-entry as well. For that purpose, newt and murine myotubes were incubated with Trichostatin A (TSA), which inhibits class 1 and class 2 HDACs, and Valproic acid (VPA), which inhibits preferentially class 1 HDACs. Analysis of the results of these initial treatments revealed an unexpected outcome: the myotubes developed constrictions between the nuclei giving them a beads-on-a-sting appearance. Interestingly, HDAC inhibitor treatment had a greater impact on murine myotubes than on newt myotubes (see Fig. 14). Furthermore, quantifications of mononucleated, MHC-positive cells demonstrated a significant difference between treatments with TSA and VPA. The percentage of mononucleated, MHC-positive cells

was up to four times higher in TSA-treated cell samples compared to VPA treatment (see Fig. 14). This was an indirect measure of cellularisation occurring.

In control experiments it was shown that HDAC inhibition does not induce MHC expression in myoblasts. This result led to further experiments with HDAC inhibitors. Considering these results, it was decided to investigate the effects of TSA on murine myotube cellularisation in more detail.

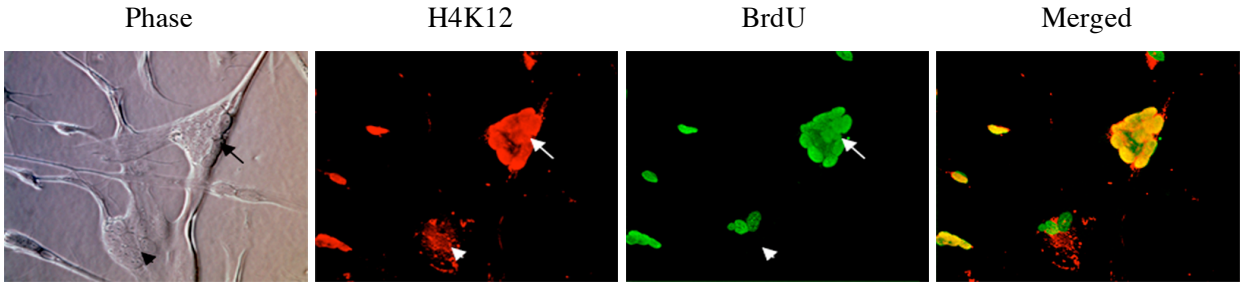

Figure 13. Cell Cycle Re-entry of Newt Myotubes Correlates with Histone Acetylation

Myotubes were cultured in proliferation medium, which causes cell cycle re-entry in newt myotubes accompanied with histone H4 lysine 12 (H4K12) acetylation (arrow). Quiescent nuclei are negative for histone H4K12 acetylation (arrowhead).

(Adopted from Dr. Andras Simon, Karolinka Institutet, Sweden)

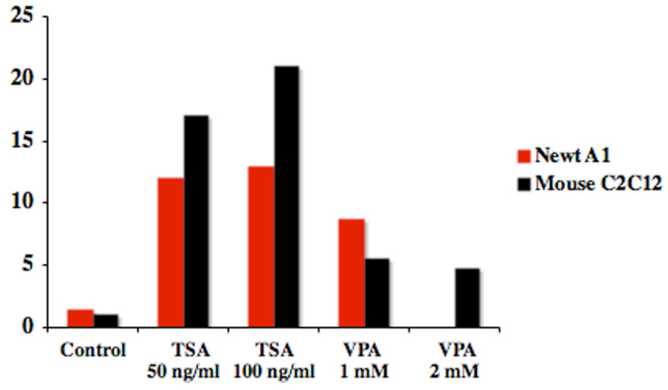

Figure 14. Statistical Evaluation of the Comparison of Trichostatin A (TSA) and Valproic Acid (VPA) treatment on Murine- and Newt Myotubes.
Columns represent percentage of mononucleated MHC-positive cells.

(Adopted from Sara Lööf, Karolinka Institutet, Sweden)

Thus, the TSA incubation studies were concentrated on murine cells. Another very important reason was the relevance in the field of regenerative medicine. Due to the relatively close

phylogenetic relationship of mouse and men it is possible that studies on murine cells can improve the knowledge of the plasticity of the differentiated state in humans as well. This would lead to a better understanding of tissue regeneration and cancer appearance and could offer new strategies for therapeutic treatments as a long term goal.

The initial experiments were carried out with mesh purified myotubes (see Material and Methods) resulting in high contamination with residual myoblasts which was unsuitable for the intended experiments. Therefore, it was necessary to get very pure myotubes. This could be achieved by the picking procedure (see Material and Methods). After picking the myotubes, cultures contained very little myoblast contamination. With these cultures the previously described experiments were repeated. The challenge thereby was that the myotubes were transferred to a totally new microenvironment by picking, as the myotubes were now sparsely seeded without contact to each other. In comparison to mesh purified cell cultures, the overall number of myotubes per dish was considerably reduced after purification by picking. The evaluation of the experiments was additionally aggravated by the fact that myotubes purified by picking are quite instable in culture and have an average lifespan of only five to seven days. It was not known whether these altered conditions would have an effect on the results of the experiments.

The initial TSA-incubation studies on mesh purified myotubes identified 100 ng/ml as an optimal concentration of TSA for the examination of cellularisation-plasticity of terminally differentiated cells, such as myotubes. Due to the altered culture conditions after picking-purification the TSA concentration was reduced to 50 ng/ml. The impact of TSA on the myotubes was analysed in comparison to control cell populations that were not incubated with TSA. As a considerable number of cells died in the TSA-treated cell populations, the concentration of TSA was then considerably reduced.

Although the number of mononucleated MHC-positive cells did not increase compared to the control well (see Table 2), there was a difference in the overall cell size. The cells in the TSA incubated wells were smaller and contained less nuclei. Unfortunately, a certain fixed number of nuclei per cell as a reliable indicator of dedifferentiation could not be defined. The arbitrarily defined amount of five or less nuclei per cell revealed no difference between TSA treated and control wells.

Increased concentrations of TSA together with longer incubation times result in increasing amounts of MHC-positive cell progeny containing fewer nuclei compared to untreated cell populations (as indicated by results summarised in Table 2). On the other hand, the overall cell number decreased dramatically the higher the TSA concentration was. Best results with respect to residing cells were achieved at a concentration of 5 ng/ml TSA for 48 hours.
Whereas the number of cells containing five or less nuclei was not increased by incubation with 5 ng/ml TSA for 48 hours, the effect on cell size and morphology was considerable (see Fig. 10). Thus, all further experiments were carried out with 5 ng/ml TSA for 48 hours if not indicated otherwise.

To date it is unknown in which way and to which extent cellularisation and cell cycle re-entry depend on each other (see Fig. 3). Nevertheless, both events occur during the reversal of the differentiated state. BrdU incorporation experiments should help to elucitate this interdependence. The results obtained so far suggest that fragmentation occurs without cell cycle re-entry as no MHC- and BrdU- double positive cells could be detected. This observation was confirmed by results of time-lapse studies where the budding of a single nucleus from the syncytium could never be observed.
The budding of a single nucleus would imply that this nucleus has become mitotically active. This may reflect the exit from the "differentiated environment" of the syncytial myotube to produce mesenchymal-like cells exhibiting stem cells properties during limb regeneration.
This result was contrary to the initial considerations where an impact of TSA exclusively on cell cycle re-entry was expected. When fragmentation occurs in the absence of cell cycle re-entry (and further in the absence of a supposed nuclear reprogramming), the observed event of fragmentation under TSA influence is supposably caused by the inhibition of HDAC 6. Zhang et al., (2003) reported that HDAC 6, a member of class 2 HDACs, is associated with the microtubule cytoskeleton (Zhang et al., 2003). Therefore, inhibition of HDAC 6, which is a target of TSA but not VPA, in muscle cells may lead to instability of the microtubule cytoskeleton and promote fragmentation into smaller progeny. This would also explain the greater impact of TSA on cellularisation described above. Furthermore, this hypothesis is consistent with the results of Duckmanton et al., (2005). Their study on fragmentation of myotubes was based on the use of a small triazine compound. Accordingly, the mere disruption of the microtubule cytoskeleton

causes cellularisation. The inhibition of protein synthesis by 10 μM anisomycin did not alter this outcome and neither was BrdU incorporated during the process of cellularisation. However, it remains unclear to which extent the different results of Duckmanton et al., (2005) can be compared to our data because different murine cell types were used for each experiment.
Thus, nuclear reprogramming is not necessary for fragmentation. Consequently, one possible way how fragmentation/cellularisation can be achieved was identified whereas the underlying regulatory mechanisms remain unclear. However, fragmentation/cellularisation is only one aspect of dedifferentiation as indicated in Fig. 4.

The results from time-lapse microscopy were consistent with the results gained from classical static microscopy. None of the 90 movies showed the formation of mononucleated offspring. The observed results did not vary, even when different media were used (see Material & Methods). One reason for this result could be that the purified myotubes adopted an unnatural conformation. In vivo, myotubes are elongated, roundish and unbranched with pointed tips at each end. In vitro, they became flattened, broad and branched. Maybe the use of different culture conditions, e.g. 3D matrix, or even a different cell type, e.g. pmi28 (Duckmanton et al., 2005) would render it possible to study the process of fragmentation in a situation more similar to the in vivo state. It is possible, that the cells in that case would react differently to the TSA treatment and budding of mononucleated progeny could occur.
As all cell progeny died after a transient resting period we wanted to investigate whether apoptosis or necrosis occurred following fragmentation. This question was interesting for two resons:
First, if the cells died necrotically then fragmentation was harmful to cultured myotubes.
Second, if the cells died by the apoptotic mechanism, further questions had to be answered: Was apoptosis the consequence of fragmentation? Or were apoptotic pathways already active before the fragmentation process set in?
In the case of an active apoptotic machinery before the start of fragmentation it would be interesting to know if certain apoptotic mechanisms are essential for the process of dedifferentiation. This hypothesis is based on observations indicating that apoptotic pathways, in particular active caspase 3, seem to be important to maintain the pluripotent potentials of stem

cells (Zwaka et al., 2005). Due to the fact that this experiment was in its initial phase by the end of this diploma work, no conclusions could be drawn, so far.

However, the data demonstrated that muscle cells undergo fragmentation in response to TSA. Because of the methodology used in this study, namely the manual picking of individual myotubes (instead of the commonly used filter method; see Material and Methods), we could show that fragmentation sets in already at very low concentrations of TSA. This points to a direct involvement of chromatin structural changes in the early aspects of dedifferentiation and provides opportunity for further detailed investigation of the dedifferentiation mechanism.

6. Material and Methods

6.1 Cell culture

6.1.1 Cell culture systems

C2C12-G myoblasts (mouse myogenic cell line derived from satellite cells) constituted the system to study the process of dedifferentiation of mammalian cells. Only cells with a low passage number were used. For high passage number derived cells have a reduced ability to differentiate, which is the main prerequisite for using them in subsequent experiments.

In order to study the urodele dedifferentiation process in vitro, A1 cells were used. Cells were obtained from Brockes, Jeremy P., University College London. Passage numbers of these cells, compared to the C2C12 cells, were much higher, around seventy.

Both cell types were stored in liquid nitrogen until usage.

6.1.2 Thawing of A1 and C2C12 cells

The thawing procedure for A1 and C2C12 cells is the same except that A1 cells require a 25˚C environment whereas C2C12 cells require a 37˚C environment. Briefly, cells were frozen in proliferation medium containing 10% dimethyl sulfoxide (DMSO). Liquid nitrogen frozen cells were thawed in a water bath. The thawed cells were transferred into fresh pre-warmed proliferation medium and subsequently spun down at 350 rpm for 10 minutes. The cell pellet was resuspended in 10 ml proliferation medium and seeded in a 165 cm^2 flask, which was already filled with 10 ml of the corresponding proliferation medium. Prior to plating A1 cells, 165 cm^2 flasks were precoated with 1% Gelatine (Sigma-Aldrich).

6.1.3 Culture conditions and passaging of C2C12 myoblasts

Cells were grown until they reached a confluency of around 60%. Depending on the experimental progress cells were passaged 1:5 to 1:10. Afterwards, media was removed, the cells rinsed twice with 10ml of prewarmed PBS and then incubated with 1.5 ml of prewarmed Trypsin EDTA for 5 minutes at 37˚C. Upon cell detachment, Trypsin EDTA was neutralized by adding 8.5 ml proliferation medium. 1 or 2 ml of cell suspension were seeded out in a 75 cm^2 flask with 9ml of proliferation medium.

C2C12 proliferation medium: DMEM ≥ 12% foetal bovine serum (FBS)

DMEM (+ 4500mg/l Glucose, + L- Glutamine, + Pyruvate) (Gibco)	85.5%
FBS (Gibco)	12.5%
Penicillin/Streptomycin (Gibco)	1%
GlutaMAX I (100×) (Gibco)	1%

C2C12-Trypsin

Trypsin EDTA (10×) (Gibco)	10%
PBS	90%

PBS: 1× D- PBS (phosphate buffered saline) (Gibco)
Had been used in all experiments.

6.1.4 Culture conditions and passaging of A1 myoblasts

A1 myoblasts were passaged in the same way as C2C12 cells. Due to the decreased growth rate of A1 cells, the need for passaging was not as frequent as for C2C12 cells. Cell culture flasks were coated with 1% Gelatine as described previously. After trypsinisation, 5ml of cell suspension were transferred to a 162 cm^2 flask containing 20 ml of A1 proliferation medium.

Media and solutions used in A1 cultures were diluted with 24% ddH_2O due to their lower osmolarity.

A1 proliferation medium: AMEM (amphibian minimal eagle medium) ≥ 12% FBS

MEM (+ Earle's, - L- Glutamine) (Gibco)	60.5%
FBS (Gibco)	12.5%
Penicillin/Streptomycin (Gibco)	1%
GlutaMAX I (100×) (Gibco)	1%
Insulin (1 mg/ml) (Sigma)	1%
ddH_2O	24%

A1-Trypsin

Trypsin EDTA (10×) (Gibco)	10%
PBS	66%
ddH_2O	24%

A1-PBS

1× PBS (Gibco)	76%
ddH_2O	24%

6.1.5 Differentiation assay

In order to study the dedifferentiation of terminal differentiated myotubes the C2C12 and A1 myoblasts had to be fused to result in multinucleated cells expressing late muscle differentiation markers like myosin heavy chain (MHC) and muscle creatine kinase (MCK). In culture this could be achieved by withdrawal of serum on confluent progenitor cells (myoblasts).

Basically, the procedure is the same for both cell-types being used. Differences arose from the different lineage. Briefly, cells were grown on cell culture dishes, coated with 1% gelatine in the case of C2C12 cells. For A1 cells coating was done with Laminin (Sigma-Aldrich) (diluted 1:100 in serum-free medium) for at least 1 hour and 1% gelatine.

When they reached confluency, the proliferation medium was removed. Cells were rinsed once with differentiation medium and subsequently cultured in differentiation medium.

Differentiation to get terminally differentiated C2C12 cells took four days. Within this time the differentiation medium was changed with a fresh one every day. The removed differentiation

medium was filtered through a syringe filter with a 0.20 µm SFCA membrane (Corning) and saved as conditioned medium.
A1 cells corresponding to their slower cell physiology took six days to yield in terminally differentiated myotubes. The differentiation medium was not changed during that time.

Differentiation medium of C2C12 cells: DMEM 1% horse serum

DMEM (+ 4500mg/l Glucose, + L- Glutamine, + Pyruvate) (Gibco)	97%
Horse Serum (Gibco)	1%
Penicillin/Streptomycin (Gibco)	1%
GlutaMAX I (100×) (Gibco)	1%

Differentiation medium of A1 cells: AMEM 0.5% FBS

MEM (+ Earle's, - L- Glutamine) (Gibco)	72.5%
FBS (Gibco)	0.5%
Penicillin/Streptomycin (Gibco)	1%
GlutaMAX I (100×) (Gibco)	1%
Insulin (1 mg/ml) (Sigma)	1%
ddH_2O	24%

6.1.6 Purification of myotubes

i) Picking assay

For C2C12 myotubes and A1 myotubes the procedure is the same, except for the cell-type specific mediums.
In order to yield the highest possible purity of myotubes the picking approach was used. Picking means that the myotubes got aspired by a glass-capillary from a cell suspension. The cell suspension contained both myoblasts and myotubes. It was possible to perform the assay manually because the size difference between mononucleate myoblasts and multinucleate myotubes was obvious.
Certain preparations were necessary before the actual picking procedure:

Coating of 24 well plates or 35 mm dishes, dependent on the consecutive application, with fibronectin (Sigma-Aldrich) (1:100 in serum-free medium) for at least 1 hour and 1% gelatine.
Furthermore, 60 mm dishes, from where the myotubes were picked, and the glass-capillaries into which the myotubes got aspired were coated with horse serum to prevent the myotubes attaching to their surface. This is important because the myotubes were meant to be transferred into the 24 well plates or 35 mm dishes mentioned above. The horse serum coated 60 mm dishes were stored with the conditioned differentiation medium (50% removed sterile filtered differentiation medium with 50% fresh differentiation medium) in the incubator until being used.
Before the picking procedure, myoblast differentiation was carried out in 12 well plates as described previously. One well of myotubes from the 12 well plate was trypsinized. Detachment was observed under the microscope. In the case of C2C12 myotubes this was important because myotubes detach faster than the surrounding myoblasts. However, there was no difference in the detachment of A1 myotubes compared to A1 myoblasts. Once the trypsinisation was sufficient in terms of myotubes being fully detached, cells were transferred to one 60 mm dish and stored in the incubator. From this point on a time window of 30 minutes was left to pick the myotubes until the death rate increases significantly. Purified myotubes were transferred into fibronectin and gelatine coated wells (see above), which contained conditioned differentiation medium.

A short description of the "picking-apparatus": The tip of the glass-capillary was trimmed to an appropriate diameter with a sterile scissor under a microscope. Now the capillary got fixed to a support. The support was placed next to an inverted microscope (Nikon Corp.) that was used for visualisation of the cell suspension and the tip of the glass-capillary during the picking procedure. Further the support was adjustable in all three space dimensions, manually. A flexible tube served as a connection between the glass capillary and a micro-volume syringe (Hamilton).
Once the cell suspension was transferred to the 60 mm horse serum coated dish (see above) the actual purification could start. The dish was placed under the inverted microscope and the plane of focus was adjusted to the level of the floating cells. Afterwards the tip of the glass-capillary was dipped into the medium of the cell suspension. The tip was placed into the centre of the visual field of the microscope and just above the floating cells. At that position the tip and the aspirated cells could be seen clearly. For aspiration of the cells the undertow from the connected micro-volume syringe was used.

ii) Mesh purification of myotubes (procedure is the same for C2C12- and A1 myotubes)

Again, this technique used the morphological feature of different size from myotubes to separate them from their progenitors. But the success rate in terms of purity compared to the picking assay was much lower.

For this assay, myoblasts were grown to confluency in 100 mm dishes scored with a scalpel to form a grid. This prevented myotubes from becoming too large. After the incubation time in the corresponding differentiation medium myotubes were purified as follows. Basically, cells were trypsinized as described above and the cell suspension was sieved through a 100 μm nylon cell strainer (BD Falcon). This step removed the big clumps of cell aggregations that were left after treatment with Trypsin. The supernatant containing myotubes as well as mononucleated myoblasts, was sieved through a 20 μm mesh (Spectrum Laboratories). In this step the myotubes were retained on the mesh whereas the small myoblasts passed through. The myotubes on the mesh were washed off by rinsing the mesh in a dish containing conditioned differentiation medium and had been coated before with horse serum, as mentioned previously. The obtained cell suspension was further separated on 24 well plates or 35 mm dishes coated with fibronectin and gelatine.

In almost all experiments done during the diploma thesis the picking assay was used.

6.1.7 Trichostatin A (TSA) treatment approach

Trichostatin A (Sigma-Aldrich) is a histone deacetylase (HDAC) inhibitor that inhibits the members of class 1 and class 2 HDACs.

Myotubes, which were isolated by picking, were allowed to attach to the substrate over night. Approximately 50% of the purified myotubes died during the first night. That was presumably an effect of stress caused by the picking procedure. Therefore, medium with the detached dead myotubes was removed and replaced by fresh, conditioned differentiation medium (see Section 6.1.5). TSA was added to the fresh, conditioned medium. Concentrations ranging from 5 ng/ml to 150 ng/ml were used.

6.1.8 5-Bromo-2'-deoxyuridine (BrdU) labeling assay

Incorporation of BrdU into DNA occurs during the S-phase of the cell cycle. For that reason BrdU incorporation can be used as a measurement to see if the cells have traversed G1/S-phase transition and started to replicate their genome.
In the approach used in this study, BrdU labelling was done after a previous TSA treatment. TSA concentration of 50 ng/ml was used. After an incubation period of 24 hours the TSA containing conditioned differentiation medium was replaced. Cells were washed once with medium containing 1% horse serum to get rid of the remaining TSA. Subsequent incubation was done with conditioned proliferation medium (75% recycled, sterile filtered proliferation medium with 25% fresh proliferation medium) containing 10 μM BrdU for 8, 16 and 24 hours, respectively, until fixation.

6.1.9 Measurement of active caspase 3

Detection of active caspase 3 in cells serves as indicator for apoptosis. Apoptosis is referred to as programmed cell death. A cascade of apoptotic-specific enzymes has to become activated to yield in apoptosis. One of these enzymes is caspase 3 which capture a central role within the apoptotic enzyme cascade. That means, if the active form of caspase 3, referred to as p17, is detected the cell is committed to undergo cell death.
In this study active caspase 3 identification was used to assay if incubation of C2C12 myotubes with TSA leads to cell death. For that purpose myotubes were purified as described in Section 6.1.6 with the picking procedure. The following day, cells were incubated with 5 ng/ml TSA for 48 hours and fixed afterwards.
For positive control cells were isolated in the same way. On the next day, cells were washed once with medium without serum to get rid of the remaining serum. Subsequently, cells were incubated in medium without serum containing 0.5 mM Staurosporine (Sigma-Aldrich) for 4 hours till fixation.

6.2 Immunocytochemistry

This method makes use of an antibody specific for the antigen of interest (primary antibody) in conjunction with a labeled second antibody (hereafter referred to as secondary antibody). This secondary antibody binds the primary antibody and can either be linked to a fluorophore directly or to biotin, which can be visualized via amplification of the signal. In both cases the goal is to make the primary antibody and hence the molecule/protein of interest visible.

Within the time of the thesis, according to the primary antibody used, different protocols were used. But in each case the secondary antibody was an Alexa Fluor conjugated antibody (Molecular Probes) raised in goat against various sources of primary antibody (Alexa Fluor 488, Alexa Fluor 546 and Alexa Fluor 633).

i) Myosin heavy chain (MHC) immunocytochemical staining

Purified, in TSA incubated myotubes (see Sections 6.1.6 and 6.1.7) were washed once with 1× PBS and prefixed to the bottom of the dish with 2% paraformaldehyde (PFA)/PBS for 1 minute at room temperature (RT). Prefixed cells were washed once with PBS followed by 5 minutes incubation in -20˚C methanol. The methanol treatment is thought to fix and permeabilize the cells. Afterwards cells were washed twice with PBS and incubated in blocking buffer (10% goat serum in PBS) for 10 minutes. As primary antibody, a mouse monoclonal anti-myosin heavy chain IgG (MF-20; Developmental Studies Hybridoma Bank) 1:200 in blocking buffer was used. Incubation was done on a shaker over night at 4˚C. Next the cells were washed three times for 5 minutes in blocking buffer. This was followed by the incubation with the secondary antibody (1:500 in blocking buffer) on a shaker for 1 hour at RT. Afterwards, the cells were washed with blocking buffer for 10 min. The nuclei got stained with 4', 6-diamidino-2-phenylindole (DAPI) (Sigma-Aldrich) at a concentration of 10 μg/ml for 2 minutes. Finally the cells were rinsed once with PBS and afterwards stored in PBS at 4˚C.

ii) MHC and BrdU double immunocytochemical staining

Cells exposed to TSA followed by BrdU incubation (see Section 6.1.7 and 6.1.8) were washed once with PBS and prefixed with 2% paraformaldehyde/PBS for 20-30 seconds at RT. Subsequently, the cells were washed once with PBS and fixed and pre-permeabilized for 5 minutes in -20˚C methanol. Again they were rinsed with PBS. In order to permeabilize the nuclear envelope to allow for BrdU staining, cells were treated with 2M HCl for 10min. Afterwards cells got washed three times with PBS and were incubated for 10 minutes in blocking buffer (10% goat serum in PBS). Incubation of primary antibody rat monoclonal anti-BrdU IgG (AccuSpec) 1:200 and primary antibody mouse monoclonal anti-myosin heavy chain IgG (MF-20; Developmental Studies Hybridoma Bank) 1:200 in blocking buffer was done simultaneously on a shaker over night at 4˚C. The primary antibodies were washed off by rinsing the cells with blocking buffer three times for 5 minutes. As secondary antibodies Alexa Fluor 488 goat anti-mouse and Alexa Fluor 546 goat anti-rat, 1:200 in blocking buffer were used, respectively. They were incubated for 1 hour at RT. Then cells got washed for 10 minutes in blocking buffer. The nuclei were stained in the same way as described for single MHC staining (see above). Staining was completed by rinsing once in PBS. Cells were stored in PBS at 4˚C until analysis.

iii) Immunocytochemical staining against activated caspase 3

Myotubes cultured with Staurosporin in medium without serum (positive control) or TSA (see Section 6.1.9) were carefully washed once with PBS. Subsequently, myotubes were fixed in 4% paraformaldehyde/PBS for 20 minutes at RT. Paraformaldehyde/PBS was removed by washing the cells for 30 minutes in PBS. The myotubes were permeabilised with 0.1% Triton X-100 (Sigma) in 0.1% tri- Sodium citrate dihydrate (Merck) for 3 minutes on ice. The citrate method removes soluble proteins from the cell nuclei. Afterwards, cells were washed in PBS three times for 5 minutes. Then the cells got blocked in blocking buffer (2% BSA in PBS) for 2 hours. Primary antibody rabbit polyclonal anti-human/mouse caspase 3 active IgG (R&D Systems) was used at a final concentration of 0.3 μg/ml in blocking buffer, incubated over night at 4˚C. Washing three times in PBS for 5 minutes followed. Secondary antibody staining using again Alexa Flour conjugated antibody (1:400 in blocking buffer) was done for 1 hour at RT. Nuclei

were stained with DAPI (Sigma-Aldrich) 10 μg/ml for 2 minutes. After rinsing once in PBS cells were stored in PBS at 4˚C.

6.3 Lineage tracing by microinjection of A1 myotubes

Microinjections were performed in order to trace myotubes.

In general, lineage tracing is the method of choice to mark and follow a specific type of cells e.g. during development. This can either be achieved by transfection of a zygote with a reporter gene that is under the control of a cell type specific promoter. In this case the reporter gene is only expressed in cells/tissues where the promoter is activated by transcriptional activators specific for the identity of the cells/tissue.
Or tracing is done in already differentiated cells. The challenge at this is that the nuclear envelope is continuously intact. To overcome this, cells can either be infected with a lentivirus that carries the reportergene or the DNA is directly injected into the nucleus.
Furthermore, specific molecules with self fluorescing properties or attached to fluorochromes can be injected into the cytoplasm to mark the cell of interest.

In this study different dyes and staining methods were applied, that shared a common modification, namely the attachment of a nuclear localisation signal (NLS) to traverse the nuclear envelope.
The NLS peptides used were a simian virus 40 T antigen NLS (NH_2 –PKKKRKVEDPYGGC-COOH) and polyomavirus large T antigen NLS (NH_2 –CGYGVSRKRPRPGC-COOH). Both were synthesized by Thermo Electron Corporation (Germany). Previous independent experiments with both peptides confirmed their functionality.

6.3.1 High molecular weight dextran

Dextrans are hydrophilic polysaccharides and characterized by good water solubility, low toxicity and relative inertness. The crucial feature for the performed experiment was that it could not cross the plasma membrane and stain surrounding cells. The dextran was already conjugated to a

fluorescein with approximate absorbance maximum at 496 nm and approximate fluorescence emission maxima at 524 nm (Molecular Probes) and was further modified by a Sulfo-SMCC linker (Pierce) with a covalently attached NLS (see above). This yielded the final construct that got injected into the A1 myotubes.

6.3.2 Reporter gene expressing plasmids

The second tracing approach applied comprised the injection of Plasmids that carried reporter genes. Two different types of constructs were used. Both had a CMV promoter to force expression of the reporter gene (see Fig. 15). While one construct carried a red fluorescence protein (RFP), the second contained a yellow fluorescence protein (YFP) tagged to a Histone 2B (H2B) - sequence. The RFP-protein stained the cytoplasm whereas the YFP-H2B-construct stained the nuclei because the fusion-protein got integrated into the nucleolus.
Both plasmids were modified with a NLS sequence, whereas the NLS peptide was not covalently linked to the plasmid. The approach applied, used a phenomenon that appears when NLS peptides are in a much higher concentration compared to the plasmid. In this case, weak molecular bond formations occur between the NLS peptides and the plasmids. These are stable enough to yield a sufficient tracing effect.

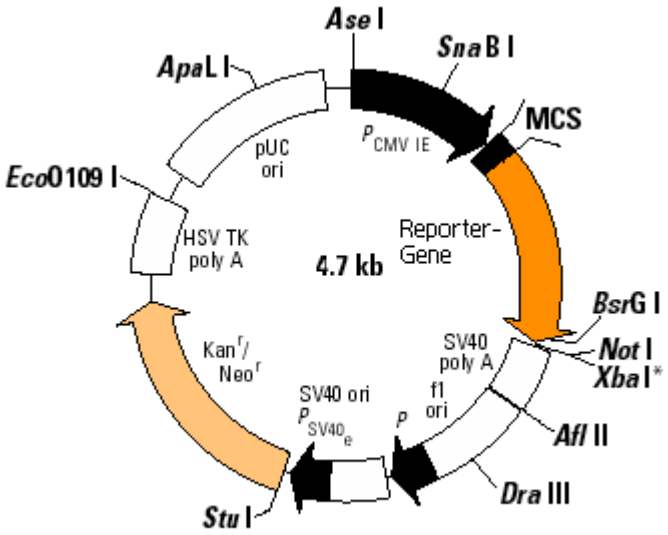

Fig 15. Schematic Diagram of the Plasmid Backbone Used for Injections of A1 Myotubes

This vector uses a CMV promoter to force expression of the reporter-gene of interest. Previous independent studies revealed that a CMV promoter is sufficient for expression in A1 myotubes. The H2B-YFP-fusion-construct was cloned into the multiple cloning site (MCS) located between the promoter and the reporter gene. The obtained H2B-YFP fusion protein traced the nuclei of the injected A1 myotubes. The same backbone but with a red fluorescence protein (RFP) as the reporter gene, served to stain the cytoplasm of the injected A1 myotubes.

6.3.3 Microinjections of A1 myotubes

Both tracing techniques (either with high molecular dextran or with the plasmids) were operated in the same way. An Eppendorf Femtojet (Eppendorf AG) in combination with an Eppendorf Injectman (Eppendorf AG) was used for injections. The injections had to be done outside the incubator, resulting in a temporal limitation of 30 minutes per plate and injection.
The actual injections were carried out with Sterile Femtotips II (Eppendorf). Back pressure between 30 and 40 hPa were sufficient to load the myotubes with approximately 750-1000 plasmid-copies/time.
Microinjections were done on A1 myotubes. For that purpose A1 myoblasts were seeded in 35 mm dishes coated with fibronectin and gelatine (as described previously). Furthermore, a grid was scored to the bottom of the dish to avoid of myotubes becoming too big. Confluent cells were induced to differentiate (see above) and microinjections were performed five days afterwards.

Subsequent to the injections cells were left to recover for one hour, after which the medium was changed. Regular differentiation medium was used, due to the fact that the myotubes were not to be isolated. Adjacent incubations were performed with TSA concentrations ranging from 10 ng/ml to 150 ng/ml. After a period of 72 hours cells were fixed for five minutes at RT by adding 4% paraformaldehyde (PFA) yielding in a final concentration of 2% PFA. Cells were rinsed once with 1xPBS and stored in PBS at 4°C until further analysis.

6.4 Animal work

All experiments were carried out according to European Community and local ethics committee guidelines. Furthermore, all animal experiments were performed either by Jamie Morrison or under his supervision. Adult red–spotted newts, Notophthalmus viridescens viridescens, were supplied by Charles Sullivan & Co (Nashville, TN, USA). Newts were kept in watertanks in a humidified room at 15- 20˚C.

6.4.1 Forelimb Amputation

Newts were anesthetized by placing them in an aqueous solution of 0.1% ethyl 3- aminobenzoate methanesulfonate salt (Tricaine) (Sigma-Aldrich) for 15 minutes. Forelimbs were amputated by cutting just proximal to the elbow and the soft tissue was pushed up to expose the bone. The bone and soft tissue were trimmed to produce a flat amputation surface. Animals were left to recover overnight in an aqueous solution of 0.5% sulfamerazine (Sigma-Aldrich) before being placed back into a 25˚C water tank. At specified time-points, the regenerating limbs were harvested after anesthetization.

6.4.2 Tissue preparation for cryosections

Initial procedures were the same as by forelimb amputations (see above).
Still anesthetized newts were sacrificed by decapitation. Harvested blastemas were embedded in Gum Tragacanth (Sigma-Aldrich). Mounted blastemas were prefrozen in liquid nitrogen-frozen isopentane (VWR) for 5 to 10 seconds. Subsequently the blastemas were transferred to liquid nitrogen and stored afterwards at -80˚C.

6.4.3 Tissue slicing

Blastemas stored at -80˚C were transferred to the cryostat (Microtome Cryostat Cryo-Star HM560M from Microm) in boxes with dry-ice. The cryostat was pre-cooled to -20˚C. Serial sections of 6 μm thickness were produced. These sections were fixed on glass slides (SuperFrost

® Plus slides from Menzel Gmbh) that had already been prepared with a positive charged surface. This was sufficient for preliminary fixation.
Tissue sections were stored at -80˚C until further usage.

6.4.4 Immunohistochemistry

Blastema tissue sections (see above) were fixed in 4% PFA for 5 minutes at RT followed by a three times washing step in PBS for 5 minutes. Afterwards, slides were incubated in 2M HCl plus 0.5% Triton X-100 (Sigma-Aldrich) for 15 minutes at 37˚C. This was followed by 10 minutes incubation in 0.1M $Na_2B_4O_7$ at RT to neutralise HCl. Subsequently, sections were rinsed in PBS 3 times for 5 minutes each. Staining was continued by blocking for 1 hour at RT. The blocking buffer consisted of 5% goat serum (DakoCytomation), 3% BSA (Sigma-Aldrich) and 0.1% Triton X-100 (Sigma-Aldrich) diluted in PBS. Afterwards, sections were rinsed once in PBS. As primary antibodies rabbit polyclonal anti-Histone H3 di-methylated K9 (ab7312) (Abcam) and a rabbit polyclonal anti-Histone H3 tri-methylated K9 (ab8898) (Abcam) were used. Primary antibodies were diluted 1/5000 in blocking buffer (see above) and incubated at 4˚C over night. Rinsing with PBS for 5 minutes 3 times each followed. For secondary antibody staining a goat anti-rabbit Alexa Fluor 488 antibody was used as usual (see previously). Again this antibody was diluted in blocking buffer (see above) to a concentration of 1/400. Secondary antibody incubation was done for 1 hour at RT. Three washes in PBS for 5 minutes followed. Next, the preparations were DAPI (Sigma-Aldrich) stained (DAPI 1/100 in PBS) for 5 minutes at RT and washed once more in PBS for five minutes. Finally, sections were mounted with fluorescent mounting medium (DakoCytomation) containing additional 100 ng/ml DAPI (Sigma-Aldrich).

Sections were stored at 4˚C.

6.5 Microscopy

6.5.1 Cell- and tissue section microscopy

Fixed and immunocytochemistry stained cells were analysed by using an inverted Axioplan 2 microscope (Carl Zeiss MicroImaging, Inc.). Phase contrast and fluorescence imaging corresponding to the secondary antibody was used.
Most pictures were taken from myotubes in the centres of wells, as usually an accumulation could be observed after purification.

Tissue sections, fixed and stained on glass slides, were analysed under an Axioplan 2 upright microscope (Carl Zeiss MicroImaging, Inc.).

6.5.2 Time-lapse microscopy

Time-lapse imaging microscopy was done with an inverted Axioplan 2 microscope (Carl Zeiss MicroImaging, Inc.). The microscope was equipped with a motorized stage. Further modifications of the microscope were an incubation chamber in combination with a CO_2 controller and a humidifier to provide a controlled environment. Cells in a 35 mm culture dish were placed in a dish holder with adjustable temperature on the stage. In this way, conditions compared to an incubator could be achieved.
Unfortunately, the initial time-lapse microscopy series had to be done with an alternative medium. This was due to the fact that the CO_2 controller was not calibrated at that time.
Thus, for the initial experiment a different incubator medium based on the L15 medium for unstable CO_2 conditions was used, until the CO_2 controller of the incubator was calibrated.

Medium for time-lapse microscopy with atmospheric CO_2 conditions

L15 (Gibco) (dissolved D $_{(+)}$ glucose to 4500mg/l)	96%
Horse serum (Gibco)	1%
Sodium pyruvate	1%
Penicillin/Streptomycin (Gibco)	1%
GlutaMAX I (100×) (Gibco)	1%

Phase contrast images were sequentially acquired through an integrated camera. Serial images were captured at each predefined stage position and focus plane on the dish every hour through a 10x or 20x objective, respectively. Limitations in the number of captured myotubes arose from the memory of the associated computer.

Isolated myotubes were kept in conditioned differentiation medium to recover over night. Directly before time-lapse microscopy the medium was changed to adjusted L15 medium (see above) or to fresh conditioned differentiation medium containing TSA (see previously). The cells were followed for a period of 72 hours. Image sequences were created from each stage position and analysed.

6.5.3 Analysis of images

All images taken during the time of the thesis were analysed using an Improvision Openlab 3.1.7 software (Improvision Ltd.). The images and image frames from the sequences were archived and further processed in Adobe Photoshop 7.0.

7. References

Bettencourt-Dias, M., Mittnacht, S., and Brockes, J. P. (2003). Heterogeneous proliferative potential in regenerative adult newt cardiomyocytes. J Cell Sci *116*, 4001-4009.

Brockes, J., and Kumar, A. (2005a). Newts. Curr Biol *15*, R42-44.

Brockes, J. P. (1997). Amphibian limb regeneration: rebuilding a complex structure. Science *276*, 81-87.

Brockes, J. P., and Kumar, A. (2002). Plasticity and reprogramming of differentiated cells in amphibian regeneration. Nat Rev Mol Cell Biol *3*, 566-574.

Brockes, J. P., and Kumar, A. (2005b). Appendage regeneration in adult vertebrates and implications for regenerative medicine. Science *310*, 1919-1923.

da Silva, S. M., Gates, P. B., and Brockes, J. P. (2002). The newt ortholog of CD59 is implicated in proximodistal identity during amphibian limb regeneration. Dev Cell *3*, 547-555.

Duckmanton, A., Kumar, A., Chang, Y. T., and Brockes, J. P. (2005). A single-cell analysis of myogenic dedifferentiation induced by small molecules. Chem Biol *12*, 1117-1126.

Echeverri, K., Clarke, J. D., and Tanaka, E. M. (2001). In vivo imaging indicates muscle fiber dedifferentiation is a major contributor to the regenerating tail blastema. Dev Biol *236*, 151-164.

Endo, T., and Nadal-Ginard, B. (1998). Reversal of myogenic terminal differentiation by SV40 large T antigen results in mitosis and apoptosis. J Cell Sci *111*, 1081-1093.

Ferretti, P., and Brockes, J. P. (1990). The monoclonal antibody 22/18 recognizes a conformational change in an intermediate filament of the newt, Notophthalmus viridescens, during limb regeneration. Cell Tissue Res *259*, 483-493.

Ferretti, P., and Brockes, J. P. (1991). Cell origin and identity in limb regeneration and development. Glia *4*, 214-224.

Finnin, M. S., Donigian, J. R., Cohen, A., Richon, V. M., Rifkind, R. A., Marks, P. A., Breslow, R., and Pavletich, N. P. (1999). Structures of a histone deacetylase homologue bound to the TSA and SAHA inhibitors. Nature *401*, 188-193.

Fraga, M. F., Ballestar, E., Paz, M. F., Ropero, S., Setien, F., Ballestar, M. L., Heine-Suñer, D., Cigudosa, J. C., Urioste, M., Benitez, J., *et al.* (2005). Epigenetic differences arise during the lifetime of monozygotic twins. Proc Natl Acad Sci U S A *102*, 10604-10609.

Gall, J. G. (1963). Kinetics of deoxyribonuclease action on chromosomes. Nature *198*, 36-38.

Gardiner, D. M., Muneoka, K., and Bryant, S. V. (1986). The migration of dermal cells during blastema formation in axolotls. Dev Biol *118*, 488-493.

Grogg, M. W., Call, M. K., Okamoto, M., Vergara, M. N., Del Rio-Tsonis, K., and Tsonis, P. A. (2005). BMP inhibition-driven regulation of six-3 underlies induction of newt lens regeneration. Nature *438*, 858-862.

Hunsinger, T. W., and Lannoo, M. J. (2007). Notophthalmus viridescens (Rafinesque, 1820)

http://www.amphibiaweb.org/cgi-bin/amphib_query?query_src=aw_search_index&table=amphib&special=one_record&where-genus=Notophthalmus&where-species=viridescens (19 July 2007 16:57 pm) (AmphibiaWeb).

Iten, L. E., and Bryant, S. V. (1973). Forelimb regeneration from different levels of amputation in the newt, Notophthalmus viridescens: Length, rate, and stages. Wilhelm Roux's Archives of Developmental Biology *173*, 263-282.

Iujvidin, S., Fuchs, O., Nudel, U., and Yaffe, D. (1990). SV40 immortalizes myogenic cells: DNA synthesis and mitosis in differentiating myotubes. Differentiation *43*, 192-203.

Jenuwein, T., and Allis, C. D. (2001). Translating the histone code. Science *293*, 1074-1080.

Johnstone, R. W. (2002). Histone-deacetylase inhibitors: novel drugs for the treatment of cancer. Nat Rev Drug Discov *1*, 287-299.

Kintner, C. R., and Brockes, J. P. (1984). Monoclonal antibodies identify blastemal cells derived from dedifferentiating limb regeneration. Nature *308*, 67-69.

Klose, R. J., Kallin, E. M., and Zhang, Y. (2006). JmjC-domain-containing proteins and histone demethylation. Nat Rev Genet *7*, 715-727.

Kumar, A., Gates, P. B., and Brockes, J. P. (2007a). Positional identity of adult stem cells in salamander limb regeneration. Comptes Rendus Biologies *330*, 485-490.

Kumar, A., Godwin, J. W., Gates, P. B., Garza-Garcia, A. A., and Brockes, J. P. (2007b). Molecular basis for the nerve dependence of limb regeneration in an adult vertebrate. Science *318*, 772-777.

Kumar, A., Velloso, C. P., Imokawa, Y., and Brockes, J. P. (2000). Plasticity of retrovirus-labelled myotubes in the newt limb regeneration blastema. Dev Biol *218*, 125-136.

Kumar, A., Velloso, C. P., Imokawa, Y., and Brockes, J. P. (2004). The regenerative plasticity of isolated urodele myofibers and its dependence on MSX1. PLoS Biol *2*, E218.

Kyrylenko, S., Kyrylenko, O., Suuronen, T., and Salminen, A. (2003). Differential regulation of the Sir2 histone deacetylase gene family by inhibitors of class I and II histone deacetylases. Cell Mol Life Sci *60*, 1990-1997.

Lachner, M., O'Carroll, D., Rea, S., Mechtler, K., and Jenuwein, T. (2001). Methylation of histone H3 lysine 9 creates a binding site for HP1 proteins. Nature *410*, 116-120.

livingunderworld.org Introduction to the Lifecycle of Newts http://www.livingunderworld.org/amphibianArticles/article0014.shtml (19 July 2007 6:00 pm).

livingunderworld.org. Notophthalmus viridescens (Rafinesque, 1820) http://www.livingunderworld.org/caudata/database/salamandridae/notophthalmus/viridescens/ (19 July 2007 6:07 pm).

Lo, D. C., Allen, F., and Brockes, J. P. (1993). Reversal of muscle differentiation during urodele limb regeneration. Proc Natl Acad Sci U S A *90*, 7230-7234.

Loh, Y. H., Zhang, W., Chen, X., George, J., and Ng, H. H. (2007). Jmjd1a and Jmjd2c histone H3 Lys 9 demethylases regulate self-renewal in embryonic stem cells. Genes Dev *21*, 2545-2557.

McGann, C. J., Odelberg, S. J., and Keating, M. T. (2001). Mammalian myotube dedifferentiation induced by newt regeneration extract. Proc Natl Acad Sci U S A *98*, 13699-13704.

Metzger, E., Wissmann, M., Yin, N., Muller, J. M., Schneider, R., Peters, A. H., Gunther, T., Buettner, R., and Schule, R. (2005). LSD1 demethylates repressive histone marks to promote androgen-receptor-dependent transcription. Nature *437*, 436-439.

Miller, O. L., Jr., and Beatty, B. R. (1969). Visualization of Nucleolar Genes. Science *164*, 955-957.

Monneret, C. (2005). Histone deacetylase inhibitors. Eur J Med Chem *40*, 1-13.

Morrison, J. I., Loof, S., He, P., Alestrom, P., Collas, P., and Simon, A. (2007). Targeted gene delivery to differentiated skeletal muscle: a tool to study dedifferentiation. Dev Dyn *236*, 481-488.

Morrison, J. I., Loof, S., He, P., and Simon, A. (2006). Salamander limb regeneration involves the activation of a multipotent skeletal muscle satellite cell population. J Cell Biol *172*, 433-440.

Murakami, T., Maki, N., Nishida-Umehara, C., Matsuda, Y., and Agata, K. (2007). Establishment of high-resolution FISH mapping system and its application for molecular cytogenetic characterization of chromosomes in newt, Cynops pyrrhogaster (Urodela, Amphibia). Chromosome Res *15*, 471-484.

Nakayama, J., Rice, J. C., Strahl, B. D., Allis, C. D., and Grewal, S. I. (2001). Role of histone H3 lysine 9 methylation in epigenetic control of heterochromatin assembly. Science *292*, 110-113.

Odelberg, S. J., Kollhoff, A., and Keating, M. T. (2000). Dedifferentiation of mammalian myotubes induced by msx1. Cell *103*, 1099-1109.

Parish, C. L., Beljajeva, A., Arenas, E., and Simon, A. (2007). Midbrain dopaminergic neurogenesis and behavioural recovery in a salamander lesion-induced regeneration model. Development *134*, 2881-2887.

Peters, A. H., Mermoud, J. E., O'Carroll, D., Pagani, M., Schweizer, D., Brockdorff, N., and Jenuwein, T. (2002). Histone H3 lysine 9 methylation is an epigenetic imprint of facultative heterochromatin. Nat Genet *30*, 77-80.

Pinou, T., Carter, A., and Stopper, G. (2000-2002a). Notophthalmus viridescens - Habitat & Ecology
http://people.wcsu.edu/pinout/herpetology/nviridescens/ecology.html (19 July 2007 5:56 pm).

Pinou, T., Carter, A., and Stopper, G. (2000-2002b). Notophthalmus viridescens-Life History
http://people.wcsu.edu/pinout/herpetology/nviridescens/lifehistory.html (19 July 2007 5:56 pm).

Rea, S., Eisenhaber, F., O'Carroll, D., Strahl, B. D., Sun, Z. W., Schmid, M., Opravil, S., Mechtler, K., Ponting, C. P., Allis, C. D., and Jenuwein, T. (2000). Regulation of chromatin structure by site-specific histone H3 methyltransferases. Nature *406*, 593-599.

Repesh, L. A., and Oberpriller, J. C. (1978). Scanning electron microscopy of epidermal cell migration in wound healing during limb regeneration in the adult newt, Notophthalmus viridescens. Am J Anat *151*, 539-555.

Repesh, L. A., and Oberpriller, J. C. (1980). Ultrastructural studies on migrating epidermal cells during the wound healing stage of regeneration in the adult newt, Notophthalmus viridescens. Am J Anat *159*, 187-208.

Riemland, S. (2000). Notophthalmus viridescens (On-line)

http://animaldiversity.ummz.umich.edu/site/accounts/information/Notophthalmus_viridescens.html (18 July 2007 4:50 pm) (Animal Diversity Web).

Rosania, G. R., Chang, Y. T., Perez, O., Sutherlin, D., Dong, H., Lockhart, D. J., and Schultz, P. G. (2000). Myoseverin, a microtubule-binding molecule with novel cellular effects. Nat Biotechnol *18*, 304-308.

Salminen, A., Tapiola, T., Korhonen, P., and Suuronen, T. (1998). Neuronal apoptosis induced by histone deacetylase inhibitors. Brain Res Mol Brain Res *61*, 203-206.

Schneider, J. W., Gu, W., Zhu, L., Mahdavi, V., and Nadal-Ginard, B. (1994). Reversal of terminal differentiation mediated by p107 in Rb-/- muscle cells. Science *264*, 1467-1471.

Shi, Y., Lan, F., Matson, C., Mulligan, P., Whetstine, J. R., Cole, P. A., Casero, R. A., and Shi, Y. (2004). Histone demethylation mediated by the nuclear amine oxidase homolog LSD1. Cell *119*, 941-953.

Simon, H. G., and Tabin, C. J. (1993). Analysis of Hox-4.5 and Hox-3.6 expression during newt limb regeneration: differential regulation of paralogous Hox genes suggest different roles for members of different Hox clusters. Development *117*, 1397-1407.

Strahl, B. D., and Allis, C. D. (2000). The language of covalent histone modifications. Nature *403*, 41-45.

Straus, N. A. (1971). Comparative DNA renaturation kinetics in amphibians. Proc Natl Acad Sci U S A *68*, 799-802.

Tanaka, E. M. (2003). Regeneration: if they can do it, why can't we? Cell *113*, 559-562.

Tanaka, E. M., Drechsel, D. N., and Brockes, J. P. (1999). Thrombin regulates S-phase re-entry by cultured newt myotubes. Curr Biol *9*, 792-799.

Tanaka, E. M., Gann, A. A., Gates, P. B., and Brockes, J. P. (1997). Newt myotubes reenter the cell cycle by phosphorylation of the retinoblastoma protein. J Cell Biol *136*, 155-165.

Thiagalingam, S., Cheng, K. H., Lee, H. J., Mineva, N., Thiagalingam, A., and Ponte, J. F. (2003). Histone deacetylases: unique players in shaping the epigenetic histone code. Ann N Y Acad Sci *983*, 84-100.

Thornton, C. S. (1938). The histogenesis of muscle in the regenerating forelimb of larval Amblystoma punctatum. J Morphol *62*, 17-47.

Velloso, C. P., Kumar, A., Tanaka, E. M., and Brockes, J. P. (2000). Generation of mononucleate cells from post-mitotic myotubes proceeds in the absence of cell cycle progression. Differentiation *66*, 239-246.

Velloso, C. P., Simon, A., and Brockes, J. P. (2001). Mammalian postmitotic nuclei reenter the cell cycle after serum stimulation in newt/mouse hybrid myotubes. Curr Biol *11*, 855-858.

Yoshida, M., Horinouchi, S., and Beppu, T. (1995). Trichostatin A and trapoxin: novel chemical probes for the role of histone acetylation in chromatin structure and function. Bioessays *17*, 423-430.

Yoshida, M., Kijima, M., Akita, M., and Beppu, T. (1990). Potent and specific inhibition of mammalian histone deacetylase both in vivo and in vitro by trichostatin A. J Biol Chem *265*, 17174-17179.

Zhang, Y., Li, N., Caron, C., Matthias, G., Hess, D., Khochbin, S., and Matthias, P. (2003). HDAC-6 interacts with and deacetylates tubulin and microtubules in vivo. Embo J *22*, 1168-1179.

Zwaka, T. P., Smuga-Otto, K., Murphy, K. R., Ludwig, T. E., Jones, J. M., and Thomson, J. A. (2005). Programmed cell death pathways are essential for maintaining pluripotency, Paper presented at: Keystone Symposia (Fairmont Banff Springs, Banff, Alberta, Canada).

8. Curriculum vitae

Name:	Geßlbauer Bernhard
Date of Birth:	13th of June 1979
Place of Birth:	Graz
Nationality:	Austrian

Education:

Since 10/2006:	Vienna University of Economic and Business Administration
10-15/09/2006:	3rd European Conference on Regeneration, Ascona, Switzerland
03/2005- 12/2005:	Diploma Thesis at Karolinska Institutet, Sweden; In the Laboratory of Prof. Dr. Andras Simon (CMB)
Since10/2002:	Vienna Medical University, Graduate Program
10/1999- 10/2008:	Vienna University: Undergraduate course in Biology with adjoining Honours course in Genetics and Microbiology
10/1998-10/1999:	Austrian Military, one-year voluntary service
06/1998:	Graduation from Military School, Wiener Neustadt, Austria

9. Acknowledgements (short and to the point)

I want to thank...

... Prof. Dr. Andras Simon for introducing me into the field of regeneration.

... my colleagues and friends from the Karolinska Institutet, especially Jamie (for my first crayfish party among other things), Anna (for talks about everything under the sun), Josh (trying to teach me English), Karolina, Frederik, and Sara for help and fun.

… Prof. Dr Franz Wohlrab (for support of various “projects” even at weekends).

... Karli “Monsieur”.

... my family and friends (eminently my grandmother and grandfather).

… Amélie.

... Lucia (without her patience this work would have never ever been finished).